

Overview: The Shape of Hadrons¹

A. M. Bernstein* and C.N. Papanicolas[†]

**Department of Physics and Laboratory for Nuclear Science
Massachusetts Institute of Technology
Cambridge, Massachusetts 02139, USA*

*†Institute of Accelerating Systems and Applications, Athens, Greece
and Department of Physics, University of Athens, Greece*

Abstract. In this article we address the physical basis of the deviation of hadron shapes from spherical symmetry (non-spherical amplitudes) with focus on the nucleon and Δ . An overview of both the experimental methods and results and the current theoretical understanding of the issue is presented. At the present time the most quantitative method is the $\gamma^* p \rightarrow \Delta$ reaction for which significant non-spherical electric (E2) and Coulomb quadrupole (C2) amplitudes have been observed with good precision as a function of Q^2 from the photon point through 6 GeV^2 . Quark model calculations for these quadrupole amplitudes are at least an order of magnitude too small and even have the wrong sign. Lattice QCD, chiral effective field theory, and dynamic model calculations which include the effects of the pion-cloud are in approximate agreement with experiment. This is expected due to the spontaneous breaking of chiral symmetry in QCD and the resulting, long range (low Q^2) effects of the pion-cloud. Other observables such as nucleon form factors and virtual Compton scattering experiments indicate that the pion-cloud is playing a significant role in nucleon structure. Semi-inclusive deep inelastic scattering experiments with transverse polarized beam and target also show the effect of non-zero quark angular momentum.

Keywords: Hadron shapes, $\gamma N \rightarrow \Delta$, QCD in confinement regime, proton deformation, pion cloud
PACS: 13.60.Le, 13.40.Gp, 14.20.Gk

PREFACE

This volume contains papers addressing issues of relevance to the broad topic of the "Shape of Hadrons". These issues were examined and debated in two meetings, which from the outset were planned to be two phases of the same workshop. The first was held at MIT in Aug. 7-9, 2004 and the second at the University of Athens in April 27-29, 2006. Many issues were raised at the first workshop and addressed at the second. The contributions contained in this volume are from the second meeting. Events did not completely conform to the original plan. Progress was more rapid due to the completion of Chiral Effective Field Theory calculations and the emergence of new, accurate data. Due to this the old questions transform themselves into new ones. At the MIT workshop an important topic was whether the effects of the pion cloud were being observed in the $\gamma^* N \rightarrow \Delta$ reaction. In the next two years the question transformed into a more precise determination of these effects.

The idea of organizing these two events grew out of a series of informal "OOPS workshops", small gatherings of a dozen or so theorists and experimentalists which occurred during the summers of 2001 and 2002 at MIT and which were focused on addressing the physics pursued by the Out Of Plane Spectrometer (OOPS) of Bates. It was realized that the field had reached a stage of maturity, where the investigation of the structure of the proton, and of hadrons in general, demanded that old questions be viewed in the light of new discoveries in related fields. New, more powerful experimental arrangements were becoming operational employing beams of superb quality and polarization. The impressive data emerging at the high end of the spectrum, at a multi GeV scale, had a bearing on the same questions but we lacked the theoretical framework to connect them. The precision of the experimental data, at least in certain sectors, had reached the stage where their interpretation was the limiting factor. Phenomenological modeling had reached a level of sophistication which allowed the distillation of key physical parameters out of a massive and diverse set of data. Theory had, for the first time, either through Lattice QCD calculations or through Effective Field Theoretical approaches, made contact to experiment. These developments needed to be understood as pieces of the

¹ This is the introductory article for the volume on the Shape of Hadrons, Athens, Greece, 27-29 April 2006 AIP Conference Proceedings, Volume 904(2007), C.N. Papanicolas, and A.M. Bernstein, editors.

same puzzle, that of the structure of hadrons. The issue of "shape" as an appealing unifying theme.

Many issues emerged clearly in the first meeting at MIT: to define precisely the meaning of "shape" for a hadron and to identify the observables that can access information concerning it; the need to understand the role of the pion cloud and of chirality (and its spontaneous breaking); to quantify the degree to which the color magnetic interaction amongst quarks can explain deformation; to understand the role of relativity; to provide the connection amongst physical quantities (such as elastic form factors, transition form factors, and polarizabilities) in determining the shape of hadrons and explaining the mechanisms that determine it. Finally, to address the elusive connection between phenomena which have driven the field at high energies (such as the EMC effect and the "spin crisis") and the low energy investigations.

In this volume these issues are raised and addressed. In this overview we attempt to provide both an introduction and a road map of how to read this volume. It is meant to be accessible, and to a certain degree, pedagogical for young scientists entering the field.

INTRODUCTION

The possibility that hadrons would have non-spherical amplitudes was first suggested by Glashow in 1979 on the basis of non-central (tensor) interactions between quarks [1]. This conjecture was based on the premise that there is a color spin-spin interaction between the quarks[2] which is modeled after the interaction between magnetic dipoles in electromagnetism ("Fermi-Breit" interaction) [3]. A few years later Isgur, Karl, and Koniuk wrote a paper "D Waves in the Nucleon: A Test of Color Magnetism" [4] which detailed an impressive list of empirical evidence for this hypothesis. In this paper they singled out the E2 transition in the $\Delta \rightarrow N\gamma$ transition as being the most definitive test of this hypothesis. Of additional interest are the quark model calculations which showed that the D state admixtures caused by the color hyperfine interaction predict a non-zero neutron charge distribution and RMS charge radius[5, 6]. These theoretical speculations induced concerted experimental and theoretical efforts to measure and calculate deviations from spherical symmetry (non-spherical amplitudes) in hadrons.

Since the proton has spin 1/2, one cannot observe a static quadrupole moment, and this has made the effort much more difficult. Since the Δ has spin 3/2, the $\gamma^*N \rightarrow \Delta$ reaction has been actively studied for non-zero quadrupole amplitudes in the nucleon and Δ . Due to spin and parity conservation in the $\gamma^*N(J^\pi = 1/2^+) \rightarrow \Delta(J^\pi = 3/2^+)$ reaction, only three multipoles can contribute to the transition: the dominant magnetic dipole ($M1$), the electric quadrupole ($E2$), and the Coulomb quadrupole ($C2$) photon absorption multipoles.

Following these initial calculations of non-spherical hadron amplitudes[4, 5, 6] there has been a considerable experimental and theoretical effort to study quadrupole transitions in the $\gamma^*N \rightarrow \Delta$ reaction (for reviews, in addition to the present volume, see [7, 8, 9, 10, 11]). Experiments have been performed with real <Kotula>²[12, 13] and virtual photons <Ungaro, Sparveris, Smith> [15]- [27]. In addition many calculations have been performed including predictions of hadron deformation <Vanderhaeghen> and reaction models which enable us to extract the resonance amplitudes from the experimental data <Drechsel-Tiator>.

In the quark model, the non-spherical D state amplitudes in the nucleon and Δ have a probability of $\simeq 1\%$ [4]. The predicted E2 and C2 amplitudes using quark models[11, 29] are much too small to explain the experimental results and even the dominant M1 matrix element is $\simeq 30\%$ low <Giannini>. A likely cause of these dynamical shortcomings is that the quark model does not respect chiral symmetry, whose spontaneous breaking leads to strong emission of virtual pions (Nambu-Goldstone Bosons)[9]. These couple to nucleons as $\vec{\sigma} \cdot \vec{p}$ where $\vec{\sigma}$ is the nucleon spin, and \vec{p} is the pion momentum. This coupling is strong in the p wave and mixes in non-zero angular momentum components. The emission and absorption of pions from the nucleon leads to the well known long range N-N tensor interaction. It was first pointed out in 1983 that the addition of virtual pions would significantly enhance the magnitude of the quadrupole amplitudes[28]. Following that, there were a number of calculations in which virtual pions were added to the quark contribution (for a review see[11]). More recently it has been shown that the shortfall of the quark models for the $\gamma^*N \rightarrow \Delta$ transition can be compensated for by the effects of the pion in dynamic models <Drechsel>[38, 39] or in chiral effective field theory calculations <Gail-Hemmert, Pascalutsa-Vanderhaeghen>[34, 33]. Nucleon charge distributions are also altered by the emission and absorption of virtual pions. For the neutron the π^-p virtual intermediate state gives rise to the observed negative square RMS charge radius, r_n^2 , since the pion tends to be at larger radii than the proton.

² All references to articles in this volume will be shown with a <bracket>. For contributions with more than two authors only the first name will be cited.

Of general interest, lattice calculations<Alexandrou> [30] show that hadrons, such as the Δ and the ρ meson are deformed. In Fig. 1 it is shown that the wavefunction of the ρ meson has a prolate shape, i.e. it extends further along the spin axis. This trend increases as the pion masses employed become lighter. For the Δ an oblate shape has been found<Alexandrou> [30]. Lattice QCD calculations have also been performed for nucleon form factors and for the $\gamma^*N \rightarrow \Delta$ transition <Alexandrou>[30]. These have been performed with large quark masses which are beyond the convergence of chiral extrapolations. The present state of the art is that, within the lattice and chiral extrapolation errors, there is rough agreement with experiment. Clearly this is an area where further work is required.

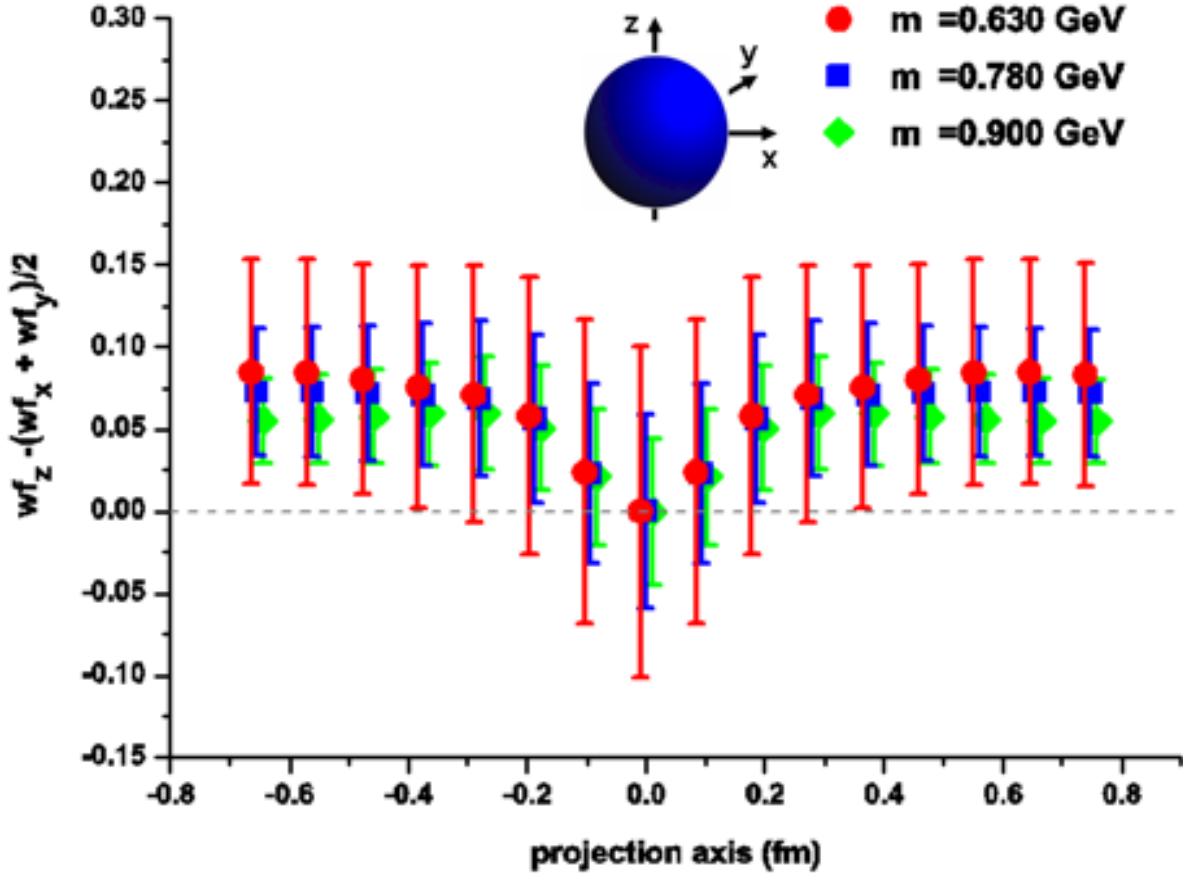


FIGURE 1. Lattice calculation of the deformation of the ρ meson<Alexandrou>[30]. The plot shows the fractional difference of the expectation value of the density along z (the spin direction) compared to the expectation in the perpendicular direction versus distance along the z axis. The calculation has been performed for three values of m_π .

In a related field, the angular momentum content of the proton measured in deep inelastic scattering has been the subject of intense experimental and theoretical activity since it was discovered that only $\simeq 25\%$ of the spin comes from the valence quarks[48]. There are concerted efforts to measure the spin contribution of the $\bar{q}q$ quark sea, the gluons and the angular momentum of the quarks. Recently, the Sivers distribution function has been measured by the HERMES collaboration and found to be non-zero <Rith> . This describes the correlation between intrinsic quark p_T and transverse nucleon spin and the result requires $L > 0$ orbital angular momentum components in the nucleon <Rith>.

There have been developments in mapping out the shape of the proton through Generalized Parton Distributions (GPD), which can be measured in deep virtual Compton scattering and hard exclusive meson production <Vanderhaeghen>. A Fourier transform of the the GPD yields a tomographic view of the nucleon, i.e. the simultaneous distribution of quarks with longitudinal momentum x and transverse position b <Kroll>. Sum rules (integrals) of the GPD's are the elastic scattering form factors[31]. It is also possible to define an $N \rightarrow \Delta$ GPD and in a similar fashion one can obtain the $\gamma^*N \rightarrow \Delta$ form factors from the appropriate integrals. These are in reasonable agreement with experiment

<Vanderhaeghen>.

Shape of Hadrons

It is worthwhile digressing to discuss the issue of shape of hadrons which is often misunderstood. The reason may be rooted in the fact that in quantum field theory, unlike non-relativistic quantum mechanics, form factors are not the Fourier transform of static densities. This is due to relativistic effects and to quantum fluctuations. At distances of the Compton wavelength ($\simeq 0.2$ fm for the nucleon) one expects classical pictures to break down. Strictly speaking, one can discuss form factors and moments of ground-state and transition amplitudes. As an example, the concept of size is straightforward since it is generally understood to mean the RMS radius of a hadron. Nevertheless, shape is a useful physical concept and can be precisely quantified in terms of ground- state or transition moments. Non-spherical distributions can be measured with the observation of quadrupole amplitudes.

The notion of shape is sometimes discussed in analogy to nuclear physics where deformed nuclei with rotational bands are well known. Somewhat closer to the present consideration would be spin 1/2 nuclei with vibrational and rotational degrees of freedom; as in the case of the proton, their static quadrupole moment of the ground state is zero. Their shape is derived through the study of their excitation spectrum. For hadrons like the proton and Δ the situation is far more complex since the constituents fluctuate (e.g. there are virtual $\bar{q}q$ pairs or mesons), relativity is important, and the system cannot be approximated as a rigid rotor. For the proton the static quadrupole moment vanishes identically on account of its spin, even if there is a probability of D states in the quark model and p states for virtual pion emission. This is an important point since we require any theory that describes these hadrons to predict these non-spherical magnitudes. The difficulty lies in the testing of these predictions because we need to study them through transitions to well described excited states. In the spectrum of the nucleon the only isolated state is the $\Delta^+(1232)$, which of course explains the intense experimental interest in the study of the $\gamma^*N \rightarrow \Delta$ reaction. Fortunately the transition from $J = 1/2$ to $J = 3/2$ with no change in parity also allows us to observe quadrupole E2 and C2 transition moments

For hadrons with total angular momentum $J \geq 1$ it is possible to measure a static quadrupole moment Q , which, if non-zero, is a clear indication of a deviation from spherical symmetry. A beautiful example of this is shown in Fig. 1 and in the figures in the contribution in this volume of Alexandrou, which shows lattice calculations for the ρ meson ($J = 1$) which is prolate ($Q > 0$, cigar like) and the $\Delta(J = 3/2)$ which is oblate ($Q < 0$, pancake like).

We can obtain an estimate of the quadrupole moment of the Δ using large N_c relations. In this case the relationship between the static quadrupole moment Q_{Δ^+} and the transition quadrupole moment $Q_{\gamma p \rightarrow \Delta^+}$ is given by [43]:

$$Q_{\Delta^+} \simeq \frac{2\sqrt{2}}{5} Q_{p \rightarrow \Delta^+} = -(0.048 \pm 0.002) \text{ fm}^2, \quad (1)$$

where the value of the transition quadrupole moment $Q_{\gamma p \rightarrow \Delta^+}$ was obtained from the empirical value of the E2 amplitude [11, 51]. This formula should be accurate up to corrections of order $1/N_c^2$. The negative value of Q_{Δ^+} supports the lattice calculation of an oblate distribution <Alexandrou>.

Since we have found that the pionic degrees of freedom are important to understand the $\gamma^*N \rightarrow \Delta$ reaction, it is instructive to discuss the shape of the nucleon and Δ in terms of an old model which allows the nucleon to emit and absorb virtual pions. This originated about 1950 to explain such phenomena as the anomalous magnetic moments of nucleons and was called the "pion atomic model" [44]. Although this model has some of the basic physics, it is only the first term in an expansion of the wave function which realistically includes multiple pions, other mesons, N^* excited states, etc. More recently the pion-cloud model has been utilized to discuss the issue of hadron shape in the context of the $\gamma N \rightarrow \Delta$ reaction [45]. In this model we describe the nucleon with spin up and the Δ (with $J=3/2$, $M=1/2$) as:

$$\begin{aligned} |N \uparrow\rangle &= \alpha |N_{core} \uparrow\rangle + \beta (-\sqrt{1/3} |N_{core} \uparrow R(r_\pi) Y_{10}(\Omega_\pi)\rangle + \sqrt{2/3} |N_{core} \downarrow R(r_\pi) Y_{11}(\Omega_\pi)\rangle), \\ |\Delta^+ \uparrow\rangle &= \alpha' |\Delta_{core}^+ \uparrow\rangle + \beta' (\sqrt{2/3} |N_{core} \uparrow R(r_\pi) Y_{10}(\Omega_\pi)\rangle - \sqrt{1/3} |N_{core} \downarrow R(r_\pi) Y_{11}(\Omega_\pi)\rangle), \end{aligned} \quad (2)$$

where the nucleon and Δ cores can be approximated as s-wave quarks. In this case the quadrupole transitions in the photo- and electro Δ excitation come from the charged pion components of the $|N_{core}\pi\rangle$ wave function which are obtained using the proper isospin Clebsch-Gordon coefficients [45]. When this is done, the spectroscopic Δ and $\gamma N \rightarrow \Delta$ quadrupole moments are found to be [45]

$$Q_{\Delta^+} = -\frac{2}{15} \beta'^2 r_\pi^2, \quad Q_{\gamma p \rightarrow \Delta^+} = \frac{4}{15} \beta' \beta r_\pi^2, \quad (3)$$

where r_π is the RMS radius of the pion distribution $R(r_\pi)$. It is interesting to see that $Q_{\Delta^+} < 0$, independent of the sign of β' , and in agreement with Eq. 1. It is also interesting to see that to have $Q_{\gamma+p \rightarrow \Delta^+} \neq 0$ both β and β' must be non-zero, i.e. the non-spherical pion-cloud must occur both in the nucleon and the Δ .

From Eq. 2 the pion density of the proton $\rho(r_\pi)$ is:

$$\rho(r_\pi) = \beta^2 R(r_\pi)^2 (1/3 |Y_{10}(\Omega_\pi)|^2 + 2/3 |Y_{11}(\Omega_\pi)|^2) \propto \beta^2 R(r_\pi)^2 (\sin(\theta_\pi)^2 + \cos(\theta_\pi)^2). \quad (4)$$

From this simple example, we see that although there are non-spherical amplitudes in the proton, proportional to β , on average it must be spherical due to its $J = 1/2$ character. As can be seen from Eq. 3 the non-spherical amplitude is observable in the quadrupole part of the $\gamma N \rightarrow \Delta$ transition.

Buchmann and Henley, in analogy to the non-relativistic case of deformed nuclei have proposed "undoing" the Clebsh-Gordon coefficients in Eq. 4 to obtain a non-spherical intrinsic pion density[45]. Once different values are substituted one can obtain either oblate or prolate shapes. Their choice gives the proton a prolate shape in its "intrinsic frame". Based on Eq. 3 the Δ is oblate. For a simple geometric picture it is probably preferable to think about the time dependence of the pion-cloud where it oscillates from the prolate $Y_{10}(\Omega_\pi)$ to the oblate $Y_{11}(\Omega_\pi)$ shape as in Eq. 4

Miller has proposed that the angular momentum content of the nucleon can be seen in a (non-relativistic) spin dependent density $\rho(r, \vec{n})$ [46, 47]

$$\rho(r, \vec{n}) = \rho(r) [1 + \vec{\sigma} \cdot \vec{n}] / 2, \quad (5)$$

where \vec{n} is the direction of the parton spin and $\vec{\sigma}$ the nucleon spin. The relativistic version of this has also been presented[46, 47]. This (non-relativistic) spin dependent density can be evaluated for the pion-cloud model of Eq. 2 for the nucleon spin in the virtual pion-nucleon state \vec{n} being parallel or anti-parallel to the nucleon spin.

$$\begin{aligned} \rho(r, \vec{n} = \vec{s}) &\propto \beta^2 R(r_\pi)^2 \sin(\theta_\pi)^2, \\ \rho(r, \vec{n} = -\vec{s}) &\propto \beta^2 R(r_\pi)^2 \cos(\theta_\pi)^2. \end{aligned} \quad (6)$$

It can be seen that the angular momentum of the πN state shows up very clearly in $\rho(r, \vec{n})$. The integral of the relativistic version of the spin-dependent density can be related to the results of spin dependent measurements in deep inelastic scattering $\Delta u, \Delta d, \Delta s$ [46, 47]. The problem (challenge) is that no experiment has been conceptualized to exhibit this density. As can be seen from the pion-cloud model, and from calculations on nucleon densities using models that fit the elastic e p scattering, there are potentially interesting spin dependent densities that can be measured[46, 47].

Last, but not least, we mention the effects of relativity on shape. As is well known, in special relativity the shapes of moving objects change when they move at high speeds. If one considers the hydrogen atom, or positronium, using the Dirac equation the small component of the wave function is in a p wave. This leads to a small, but definite, non-spherical amplitude[46, 47]. The issue of relativity for positronium is discussed in more detail using the Bethe-Salpeter equation <Hoyer>. It is shown that the Fock components have a more complex shape change under relativistic boosts than a flattening of their distributions along the direction of the boost. To our knowledge this effect has not been incorporated into quark models with current quark masses for which the relativistic aspects should be large.

THEORY AND MODELS OF NON-SPHERICAL HADRON AMPLITUDES

In the introduction the development of the field and the key ideas and calculations were presented in historical order. In this section the basis for non-spherical hadron amplitudes will be presented in somewhat more depth, primarily from the point of view of QCD. An important theoretical development of the past few years is the emergence of lattice simulations of QCD and their application to nucleon form factors and to the $\gamma^* N \rightarrow \Delta$ reaction <Alexandrou>[30]. At the present time these calculations are limited to relatively heavy quark masses by the constraints of computational ability (computer resources and technology). The calculations reported here correspond to pion masses in the range of 410 to 560 MeV for quenched and 380 to 690 MeV for unquenched calculations <Alexandrou>[30]. These masses are too high to see the pion-cloud effects and also for reliable chiral extrapolations. Unfortunately, the time required to improve these calculations goes as a high inverse power of the pion mass. Computational limitations also have resulted in relatively large statistical errors encountered in the sampling of the numbers of gauge configurations (N_g) in these calculations with the errors going as $1/\sqrt{N_g}$. In addition, the effects of employing different lattice Fermion formulations and lattice spacings must be evaluated <Alexandrou>[30]. Using chiral extrapolations, qualitative agreement with experiment has been achieved <Pascalutsa>[34]. These calculations predict significant deviations of hadron

structure from spherical symmetry (shown in Fig. 1) and in the non-zero values of the quadrupole amplitudes in the $\gamma^*N \rightarrow \Delta$ reaction. Predictions for the axial form factors in the parity violating electro-excitation of the Δ have also been made in advance of the experiments, which are to be performed at JLab. It is gratifying that calculations with pion masses as low as 250 MeV are becoming available <Alexandrou>. These will enable accurate chiral extrapolations to connect with data in a quantitative way and also allow us to better explore the pion contribution to the observables.

In the past few years theoretical calculations have progressed using chiral effective field theory <Gail-Hemmert, Pascalutsa-Vanderhaeghen>[32, 33, 34, 11]. These calculations represent the first approach to estimate QCD predictions using a perturbation expansion. The first to be published used the epsilon expansion, where $\varepsilon = \{\frac{|Q|}{\Lambda}, \frac{m_\pi}{\Lambda}, \frac{\Delta}{\Lambda}\}$ with $\Lambda = \{4\pi F_\pi, M_N\} \simeq 1\text{GeV}$ [32, 33]. These calculations of the (complex) M1, E2, and C2 transition amplitudes were carried out to order ε^3 and are in qualitative agreement with experiment as will be shown below. An alternative expansion in terms of another small parameter δ was also carried out <Pascalutsa-Vanderhaeghen>[34, 11]. In this case $\delta = \{\frac{|Q|}{\Lambda}, \frac{\Delta}{\Lambda}\}$, $\delta^2 = \frac{m_\pi}{\Lambda}$, where $\Lambda = 4\pi F_\pi$. The main difference between these calculations is that in the delta expansion $m_\pi \simeq 140$ MeV is considered significantly smaller than $\Delta \simeq 300$ MeV. In practice this means that some graphs are neglected as higher order in the δ expansion. From a theoretical perspective a significant difference between m_π and Δ is that only the former vanishes in the chiral limit, and it is argued that it should be treated on a different footing <Pascalutsa-Vanderhaeghen>[34, 11]. (Note that Δ vanishes in the large N_c limit.) The other difference is that the ε expansion has also been employed in heavy Baryon chiral effective field theory, while the δ expansion has been utilized with a relativistic version of chiral perturbation theory. Furthermore, the way that the low energy constants have been chosen is different in both calculations. It is also the case that the calculations using the δ scheme have been carried out successfully for the cross sections in the $\gamma^*N \rightarrow \Delta$ reaction. Within the estimated relatively large errors due to the neglect of higher order terms, both approaches agree with the data for the observables that have been calculated. To make further progress we need to have the next order calculations (including cross sections) for both expansions. We can then use the comparison with experiment to see if there are any significant differences between these two approaches. This is particularly important since the differences between the two calculations involve a mixture of ingredients which makes them somewhat difficult to compare purely theoretically.

The δ scheme has been used to predict a chiral extrapolation for the lattice calculations as a function of pion mass as shown in Fig.2. This has been done for m_π values from 0 up to 0.35 - 0.5 GeV where the lattice calculations were performed. Even though these values far exceed the premise of the chiral calculations that $m_\pi \ll \Delta \simeq 0.3$ GeV they produce qualitatively similar results to the calculated lattice values for the EMR= E2/M1 and CMR= C2/M1 ratios. The calculated curves show a strong dependence for $m_\pi \leq 0.35$ GeV. They also indicate that a linear dependence in m_π^2 may be accurate for the EMR but not the CMR. Using this chiral extrapolation<Pascalutsa-Vanderhaeghen>[11, 34] improves the agreement between the lattice calculations and experiment. These first results, impressive as they are, they can only be viewed as suggestive due the above mentioned limitations. They pave the way and they highlight for the need for lattice calculations with smaller pion masses and, in addition, higher order chiral calculations to make quantitative comparisons between QCD and experimental data.

As was discussed in the introduction, historically the first calculations of the deviation of hadron shapes from spherical symmetry were performed using the non-relativistic quark model[4, 5, 6]. Although the quark model is able to reproduce the spectrum of low lying excitations of hadrons, it is not able to accurately reproduce the observed transition rates[29]. In addition to the problems of not agreeing with experiment, the quark model has internal consistency problems. It has been shown that depending in the choice of gauge the size of the calculated E2 transition matrix element can differ by an order of magnitude [35]. This problem, which is a manifestation of space truncation, is particularly serious when only $2\hbar\omega$ configurations are used. Subsequent quark model calculations using up to $6\hbar\omega$ configurations were performed and showed less sensitivity to the choice of charge and current operators[29]. These calculations produced EMR ratios of $\simeq -0.4\%$ at the photon point for the non-relativistic quark model and $\simeq -0.2\%$ for the relativized quark model[29] as compared to the experimental value of $\simeq -2.5\%$. Since the value of the M1 transition is typically underestimated by $\simeq 30\%$ in quark models <Giannini>[11, 29], this makes the underestimate of the E2 matrix element even more serious. As will be discussed in the next section, the Q^2 dependence of the quark model calculations are even in more disagreement with experiment. This holds for all of the non-relativistic and partially relativized quark models.

In being able to describe low lying energy levels but not electromagnetic transition rates, the quark model is similar to the shell model of nuclei which can also reproduce the low lying spectra of excited states but requires collective effects to explain the electromagnetic transition rates. In the case of hadrons, however, the solution to the problem is quite different. The quark model does not respect the spontaneously hidden chiral symmetry of QCD which leads to the p wave emission and absorption of pions. This non-spherical πN interaction leads to greatly enhanced quadrupole

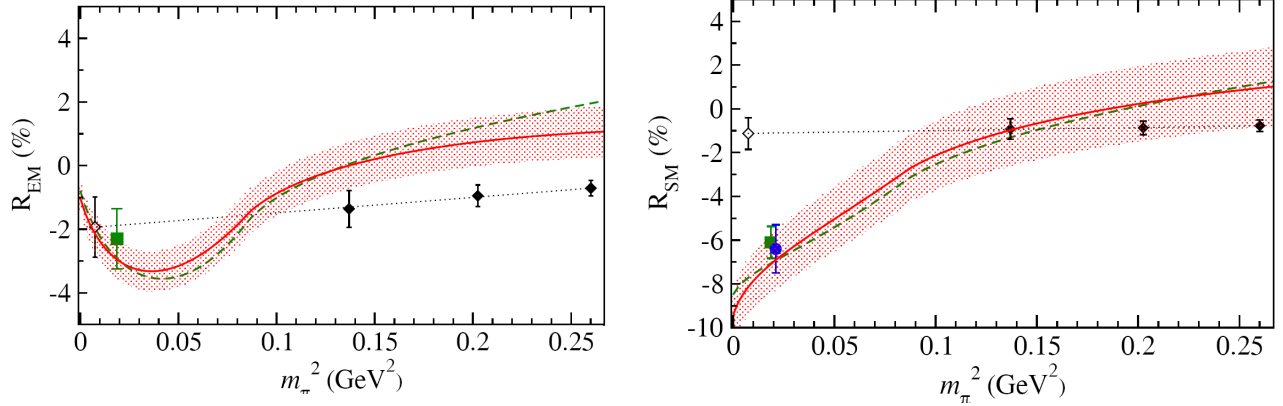


FIGURE 2. The pion mass dependence of R_{EM} (left panel) and R_{SM} (right panel), at $Q^2 = 0.1 \text{ GeV}^2$. The blue circle is a data point from MAMI[21], the green squares are data points from BATES [16, 18]. The three filled black diamonds at larger m_π are lattice calculations [30], whereas the open diamond near $m_\pi \simeq 0$ represents their extrapolation assuming linear dependence in m_π^2 . Red solid curves: NLO result when accounting for the m_π dependence in M_N and M_Δ ; green dashed curves: NLO result of <Pascalutsa-Vanderhaeghen> Ref. [34], where the m_π -dependence of M_N and M_Δ was not accounted for. The error bands represent the estimate of theoretical uncertainty for the NLO calculation. See text for discussion.

transitions in the $\gamma^* N \rightarrow \Delta$ reaction and also to the proper enhancement of the M1 transition[38, 39].

The fact that pions were needed to cure the dynamics problems of the quark model was first suggested in 1983 in the context of a cloudy bag model[28]. Subsequent calculations with chiral (cloudy) bags gave E2/M1 values of $\simeq -2.0\%$ at the photon point but with the M1 matrix element still $\simeq 30\%$ low[36]. These predictions are unstable as demonstrated by the fact that calculations with a similar model, but taking center of mass recoil into account, obtained an M1 matrix element close to experiment but reduced E2/M1 to $\simeq 0$ [37]. The pion-cloud was also shown to be able to produce E2/M1 ratios $\simeq -2\%$ at the photon point with a linear sigma model, but the magnitude of the M1 transition is $\simeq 20\%$ low[40] and the Q^2 dependence does not match experiment (for a review of the quark models and pionic extensions see [11]).

An extension of the quark model to include π and σ meson exchanges has been developed and leads to a prediction of E2/M1 $\simeq -3.5\%$ at the photon point[41]. The enhancement of the E2 amplitude comes from a two quark operator in this model. However, the magnitude of the M1 amplitude is $\simeq 30\%$ low, a value which is not improved over other non-relativistic quark models. Within this model an interesting relationship has been derived between $G_{En}(Q^2)$, the electric form factor of the neutron, and the $C2(Q^2)$ transition amplitude which is reasonably accurate empirically <Buchmann>[42]; in the low Q^2 region the transition quadrupole moment of the $\gamma p \rightarrow \Delta^+$ reaction is related to the square of the RMS radius of the neutron charge distribution r_n^2 as:

$$\begin{aligned} Q_{\gamma p \rightarrow \Delta} &= r_n^2 / \sqrt{2} = -(0.084 \pm 0.002) \text{ fm}^2, \\ Q_{\gamma p \rightarrow \Delta}^{exp} &= -(0.085 \pm 0.003) \text{ fm}^2, \end{aligned} \quad (7)$$

where the value of $r_n^2 = -0.119 \pm 0.003 \text{ fm}^2$ was taken from [52] and the experimental value of $Q_{\gamma p \rightarrow \Delta}$ was obtained [11] from the empirical value of the E2 amplitude[51]. The remarkably good agreement is impressive. Equation 7 was initially derived using the quark model[41] and subsequently in the large N_c limit <Buchmann>[43].

Pion Contribution to Hadron Properties

It is well known from deep inelastic scattering that the $\bar{q}q$ amplitudes play a large role in nucleon structure[48]. On general grounds it is expected that a significant part of this contribution will be in the long range contribution of pions. These are strongly coupled to hadrons, and due to the spontaneous hiding of chiral symmetry in QCD are emitted and absorbed in p states. This contributes significantly to the long range non-zero angular momentum amplitudes

and the observables that depend on them such as the quadrupole transitions in the $\gamma^*N \rightarrow \Delta$ reaction. However, it is not possible to quantify the contribution of the pion contribution to any observable in a model independent way <Meissner>. Qualitatively we expect that if the pion contribution to a specific observable is large, this would show up in a lattice calculation by a relatively rapid dependence on the pion mass, particularly as one approaches the physical value. Again this will be difficult to quantify using a chiral extrapolation. In chiral perturbation theory the pion loop contributions are well defined. However, there are both short range physics and pionic contributions to the low energy constants and the relative contribution cannot be obtained in a model independent way <Meissner>. These constants are either obtained by fitting chiral calculations to data or to lattice calculations. For dispersion calculations it is straightforward to identify the single pion contribution but not possible to isolate the pionic part of the empirical vector meson contributions. In the case of quark model calculations there is no pion contribution. However when empirical form factors are introduced for the dressed quarks it is not possible to identify the pionic contribution.

Despite this quantitative limitation, it is still physically interesting to qualitatively see where pionic effects are significant. For example, as has been shown above, in the quadrupole amplitudes in the $\gamma^*N \rightarrow \Delta$ reaction, quark models do not fall far short and models with pion-clouds are in qualitative agreement with the data. In such a case we can be reasonably confident that the bulk of the observed quadrupole amplitudes is due to pionic effects. As will be shown in the next section, virtual pion effects significantly contribute in virtual Compton scattering. For nucleon form factors on the other hand, as will also be discussed in the next section, there is also a significant pionic contribution at low Q^2 . However, it is difficult to exactly identify the pionic contribution. The issue of the identifying and quantifying the role of mesonic, and in particular pionic, contributions is physically interesting and important. It would be good to see some progress in the coming years.

Nucleon Form Factors and Virtual Compton Scattering

For one photon exchange processes nucleon properties cannot be directly used to demonstrate non-spherical amplitudes due to the fact that the spin of 1/2 precludes an observable quadrupole moment. However, low energy processes such as photon and electron scattering can be used to show pionic effects, which are responsible for most of the quadrupole amplitudes in the $\gamma^*N \rightarrow \Delta$ reaction at low Q^2 . In this sense any evidence for pionic effects are part of the shape of hadrons story. The importance of pionic effects can be seen from chiral perturbation theory (ChPT) calculations for the nucleon polarizabilities and isovector radii. For both of these cases these quantities diverge in the chiral limit ($m_\pi, m_u, m_d \rightarrow 0$) indicating that they are pion field dominated. It also should be pointed out that the long range tensor part of the Yukawa interaction is due to non-spherical pion emission and absorption of pions from nucleons.

In the past few years, there has been considerable progress in the measurement of nucleon electromagnetic form factors <de Jager>. There has also been considerable theoretical activity to explain these results. Of particular interest to the issue of the pionic effects on the nucleon form factors is the electric form factor of the neutron G_{En} . Intuitively, it is expected that at low Q^2 this is dominated by the virtual emission and absorption $n \rightarrow \pi^- p$. This leads to a negative RMS radius r_n^2 in agreement with experiment. It is interesting to note that if one assumes the relationship between the pion-cloud dominated transition quadrupole moment in the $\gamma p \rightarrow \Delta$ reaction and r_n^2 presented in Eq. 7, then this confirms our expectation that the long range neutron charge distribution is also pion dominated. This idea is reinforced by quark model calculations which predict quadrupole transition matrix elements for the $\gamma^*N \rightarrow \Delta$ reaction which are an order of magnitude too small <Giannini, Sparveris>[18, 24, 25]. For G_{En} the hypercentral quark model <Giannini> predicts a maximum magnitude of $\simeq 0.15$ for $Q^2 \simeq 0.3 \text{ GeV}^2$ [53] compared to the experimental value of 0.40 to 0.60 <de Jager>. This significant shortfall implies a large pionic contribution <Giannini> as in the $\gamma^*N \rightarrow \Delta$ reaction.

The status of $G_{En}(Q^2)$ is shown in Fig. 3 with the published polarization data. The curves are the latest dispersion calculation[54, 55] and a two dipole fit[58] with their (not often shown) one sigma errors. It can be seen that these are in good agreement with the data. The electric and magnetic nucleon densities can be obtained, in an approximate way, from the Fourier transform of the form factors. This interpretation is useful physically but is accurate only at long distances. For high Q^2 the recoil of the final state makes the approximation of a static density inaccurate. These errors are minimized by working in the Breit frame and the results for the neutron densities [59] are shown in the right panel of Fig.3. For the neutron charge distribution the fact that the negative charge dominates at long distances, in agreement with the negative RMS radius squared r_n^2 , is in qualitative agreement with the pion cloud picture in which $n \rightarrow \pi^- p$ part of the time.

The elastic electron scattering form factors and the $\gamma^*N \rightarrow \Delta$ transition have been calculated in a relativistic quark

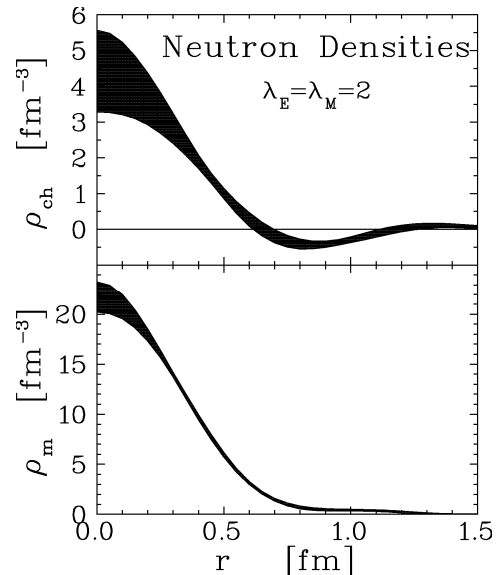
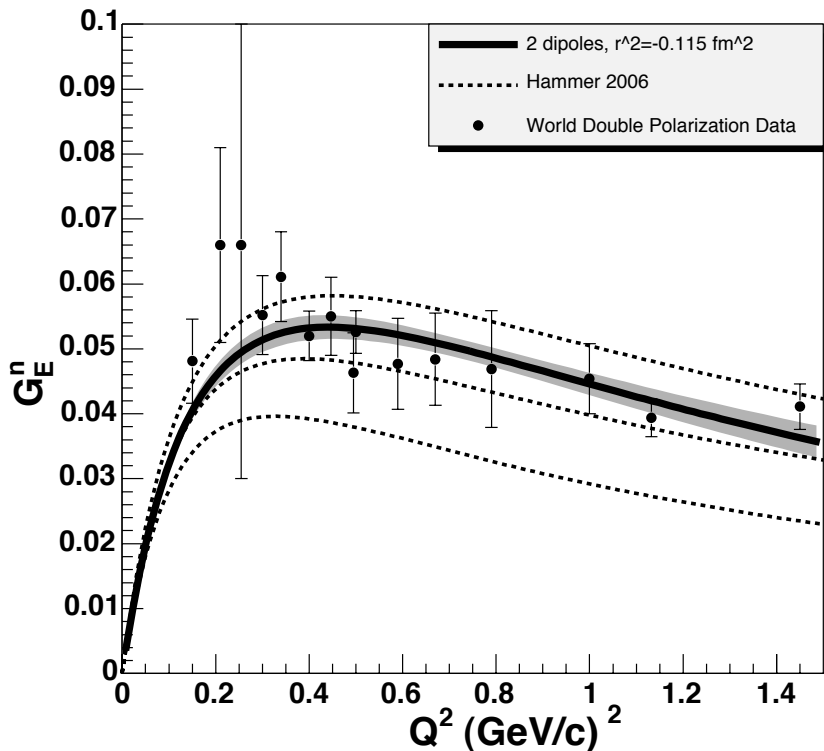


FIGURE 3. Left panel: Modern, double polarization data for $G_{En}(Q^2)$ (see <deJager> for references). The curves include the latest dispersion calculation[54, 55] and a two dipole fit[58] with their one sigma errors. Right panel: The allowable bands for the neutron electric and magnetic densities derived from the observed form factors by Kelly[59]

model, which includes a pseudoscalar meson cloud described with chiral techniques, and with additional vector meson-photon coupling[60, 61]. The model includes heavy constituent quarks with empirically determined dipole form factors (8 parameters) and current masses for the chiral part of the calculation. Perhaps with all of these parameters it is not surprising that it is in reasonable agreement with experiment. The calculated pion contribution to the form factors is found to be significant above $Q^2 = 0.5 \text{ GeV}^2$. However, this contribution is artificially suppressed by a cutoff factor $f_{cut}(Q^2)$ which is chosen to go to zero above this value. It should be pointed out that other model calculations have achieved reasonable agreement with the data with far fewer ingredients (and parameters). The hypercentral quark model has achieved reasonable fits to the form factor data (with the exception of G_{Ep} at low Q^2) by introducing empirical form factors for the constituent quarks[53]. Using vector dominance, reasonable fits to the nucleon form factors have also been achieved <de Jager>[62]. Therefore, it is not clear just what ingredients of the chiral quark model are required to achieve its good agreement for the nucleon form factors and the $\gamma^*N \rightarrow \Delta$ reaction for low Q^2 [60, 61]. Further investigation of this avenue is clearly needed in order to achieve the most economical description of the data within this framework.

It is of interest to inquire what information about the shape of the proton can be inferred from model fits to the nucleon electromagnetic form factors. Miller has done this with a quark model fit to the recent form factor data[46, 47]. Using the relativistic version of Eq.5 for the spin-dependent density the non-spherical shapes of the proton as a function of quark momenta have been calculated. These correspond to considerable angular momentum content for the proton. Recently, there have been some calculations in which S wave quark models have been used to fit the nucleon form factors[63]. In a subsequent paper it was pointed out that this model did have some non-spherical amplitudes[47].

This inspired a re-fit of the nucleon form factors with purely S wave quarks[64]. Unfortunately, due to the spin 1/2 nature of the proton there is not an unambiguous test of the validity of the angular momentum content of these wave functions in elastic ep scattering which is primarily mediated by one photon exchange. Specifically we do not have any straightforward way to measure the spin dependent densities. At this point the most straightforward test would be for both models to calculate the $\gamma^* p \rightarrow \Delta$ reaction to see if they agree with the data presented here. Of course, this will also involve a wave-function for the Δ . Another possibility, using only the proton wave function, would be to calculate the expected Sivers function for pion and kaon production <Rith>.

Another reaction which is very sensitive to the virtual pion field of the nucleon is Compton scattering with real and virtual photons. This is seen in the expression for the electric and magnetic polarizabilities in chiral perturbation theory (ChPT) which diverge as $1/m_\pi$ [66] indicating pion dominance. A new development in this field has been the completion of a virtual Compton scattering (VCS) experiment at $Q^2 = 0.057 \text{ GeV}^2$ at Bates <Miskimen>[65]. The results are in agreement with heavy Baryon ChPT to order $O(p^3)$ [67]. An interesting aspect of the Q^2 dependence of the electric polarizability $\alpha(Q^2)$ is the extraction of its RMS radius $r_\alpha^2 = 2.16 \pm 0.31 \text{ fm}^2$, which is in reasonable agreement with the ChPT prediction of 1.7 fm^2 and far larger than the RMS electric radius of the proton $r_p^2 = 0.757 \pm 0.014 \text{ fm}^2$. This also indicates a pion-cloud dominance for the electric polarizability of the proton.

Based on the spontaneous hiding of chiral symmetry, which leads to the strong p wave coupling of pions to nucleons, it is generally agreed that pionic effects play an important role in nucleon structure. This is reinforced by a large body of empirical evidence. As was discussed in the previous section, the pionic contribution is only a qualitative concept and cannot be made model independent. This was seen in particular in the discussion of the pionic contribution to nucleon form factors. There the definition of pionic effects are not the same as in the case of dispersion calculations <Meissner>[57] and in the Friedrich-Walcher empirical definition [56].

Models for the $\gamma N \rightarrow \pi N$ and $e N \rightarrow e' \pi N$ Reactions

The ideal way to compare theory and experiment for the $\gamma^* N \rightarrow \pi N$ reaction would be to start with QCD and compare the experimental observables with the predictions. The first step towards this approach has been taken with a chiral effective field theory (ChEFT) calculation to next to leading order (NLO) <Pascalutsa-Vanderhaeghen>[34]. This work also estimated the theoretical errors due to the next order (NNLO). Within these estimated errors the calculations are in reasonable agreement with experiment. Unfortunately, these errors are relatively large so that these next order calculations are required for a quantitative comparison between theory and experiment. The other QCD based calculations, lattice[30] and ChEFT <Gail-Hemmert>[33] calculate the multipoles, so that these need to be extracted from experiment.

The Δ resonance ($J = I = 3/2$) is at a center of mass energy of $\simeq 1232 \text{ MeV}$, and has a width $\Gamma \simeq 100 \text{ MeV}$ [51]. It decays $\simeq 99\%$ to the πN channel and $\simeq 1\%$ to the γ channel. Its shape and width are dominated by the πN interaction. Both photo- and electro-pion reactions are strongly linked to the πN channel by unitarity (Fermi-Watson theorem). The large width of the Δ has important dynamical implications which must be taken into account in proper dynamic calculations. Unfortunately in lattice calculations with heavy pions, quark models and pion extensions, the Δ is treated as an excited state and not part of the πN continuum[30, 28, 36, 37, 40, 41, 42]. This has the important consequence that the $\gamma^* N \rightarrow \Delta$ transition is limited by angular momentum and parity considerations to have three possible multipole amplitudes. These are the dominant magnetic dipole M1 due to quark spin flip and the electric and Coulomb quadrupole E2, and C2 amplitudes which signal the non-zero angular momentum components in the nucleon and Δ states. This represents a simplification which must be removed in a realistic analysis of the data. What is measured is the $\gamma^* N \rightarrow \pi N$ reaction initiated by real or virtual photons. Since this is a continuum final state, there are an infinite number of possible multipoles. At low energies the practical number of significant multipoles is limited to $\simeq kR$ where k is the momentum of the outgoing pion and R is the nucleon size. For energies of 1 GeV or less we expect contributions of less than 5 units of angular momentum. In addition we have to take into account the fact that there are two final charge states possible for either a proton or neutron target, which is conveniently characterized in terms of isospin.

In electro-pion production notation (see [68] for details) the three allowable Δ resonance amplitudes M1, E2, and C2 are $M_{1+}^{3/2}, E_{1+}^{3/2}, S_{1+}^{3/2}$ where the letter (M, E, S) stands for magnetic, electric, and scalar. The subscript (1+) stands for the angular momentum $L = 1$, the plus sign means that the total angular momentum $J = L + 1/2 = 3/2$. The superscript is the isospin $I = 3/2$ [68]. All other multipoles are background coming primarily from Born terms and from the tails of higher resonances <Drehssel-Tiator>. The multipoles are complex numbers which are functions of W and Q^2 . The

Fermi-Watson theorem states that the phase angle is the same as in πN scattering (a function of W only). This depends on unitarity, isospin conservation, and the fact that only the πN and γ channels are open so that it is not strictly valid above the two pion threshold. The small deviations of the Fermi-Watson theorem due to isospin breaking (e.g. by the mass difference of the up and down quarks) can be removed if the precision of the experiments warrants[69].

Reaction models of $\gamma^* N \rightarrow \pi N$ play a central role in the determination of the multipole amplitudes. None of the experiments performed to date has a sufficient number of polarization observables to perform a model independent determination of the multipoles and so models have to be utilized to extract the multipoles of interest. Typically, experiments extract the resonant multipoles $M_{1+}^{3/2}, E_{1+}^{3/2}, S_{1+}^{3/2}$ from experiment by fitting them to the data and assuming that the background (Born) amplitudes are properly described by the model. In some cases the extraction uses several models to test this hypothesis <Stave *et al.*>. The calculations that have been used in this way are the pion cloud dynamic models of Sato and Lee[38] and DMT[39]. There is the phenomenological MAID <Tiator-Kamalov>[70] and closely related calculation of Aznauryan[71], and finally the multipole fitting SAID program <Arndt *et al.*>[50]. For a fuller discussion of these calculations see <Drechsel-Tiator>. At the workshop a model independent method to extract the multipoles was presented<Stiliaris-Papanicolas>.

High Energy Probes and Generalized Parton Distributions

Inclusive deep inelastic lepton scattering (DIS) was used to determine that spin 1/2 confined quarks make up the proton and to measure their distribution functions (for a review of the data see [51]). From experimental integrals of the distribution functions it was determined that the quarks carry only $\simeq 50\%$ of the proton momentum. Later DIS measurements with polarized beams determined that only $\simeq 25\%$ of the proton spin comes from the valence quarks [48]. There are concerted efforts to measure the spin contribution of the $\bar{q}q$ quark sea, the gluons and the angular momentum of the quarks with high energy leptons, and polarized proton scattering at RHIC. These promising experimental studies are just beginning. It is believed that a significant amount of the proton spin is carried by the angular momentum of the quarks and by the gluons[48]. These high energy studies are complimentary to the main focus of this workshop, which has been on the long range part of the non-zero angular momentum amplitudes in the proton and Δ . As we have seen, these are largely due the pion (more generally $\bar{q}q$) contribution. We believe that the future work, using high energy probes, will map out the short range, quark, angular momentum amplitudes and connect the short and long range contributions. It may be possible to identify the quark structure of the pion cloud and connect parton distribution information with form factors through sum rules.

In the past few years there have been developments in mapping out the structure of the proton through Generalized Parton Distributions (GPD) which can be measured in deep virtual Compton scattering (DVCS) and hard exclusive meson production <Vanderhaeghen>. The GPDs contain information about both the spatial and momentum distribution of the quarks. A Fourier transform of the GPD yields a tomographic view of the nucleon, i.e. the simultaneous distribution of quarks with longitudinal momentum x and transverse position b <Kroll>.

In Compton scattering at high energies, two reaction mechanisms, shown in Fig. 4 have been proposed. The left hand diagram shows the initial hard real or virtual photon being absorbed by many quarks with virtual gluons mediating the interaction. The right hand "handbag" diagram shows the incident photon being absorbed by one quark. There have been two recent JLab experiments which show the dominance of the handbag diagram. One involves the polarization transfer from circularly polarized photons at $s = 6.9 \text{ GeV}^2$ and $t = -4.0 \text{ GeV}^2$ [72]. The second JLab experiment confirmed that the handbag diagram can be extracted from experiment in a deep virtual Compton scattering DVCS experiment at modest Q^2 (1.5 to 2.3 GeV^2)[73]. In the "handbag" diagram the struck quark propagates after (or before) emitting the outgoing photon so that in contrast to elastic lepton scattering, which is primarily mediated by a single photon exchange, DVCS can provide information about the angular momentum of the struck quark. The "handbag" amplitude factorizes into a hard and soft part, shown as the lower blob which represents the generalized parton distributions. We anticipate a large amount of work in this field in the coming decade.

The GPDs have been parameterized by using models and the appropriate integrals over the GPDs (one of which gives the nucleon form factors) <Vanderhaeghen, Kroll>[31, 74]. Figure 4 shows the DVCS for either the nucleon or the Δ as the final state. By taking the proper integrals of the GPDs for the $N \rightarrow \Delta$ transition, and by utilizing large N_c calculations, the form factors of the $\gamma^* N \rightarrow \Delta$ transition can be obtained and are in reasonable agreement with experiment (see Fig. 12 of <Vanderhaeghen>). Another way to look at the information obtained with GPDs is through the Wigner phase space distribution which links the spatial and momentum quark correlations[75].

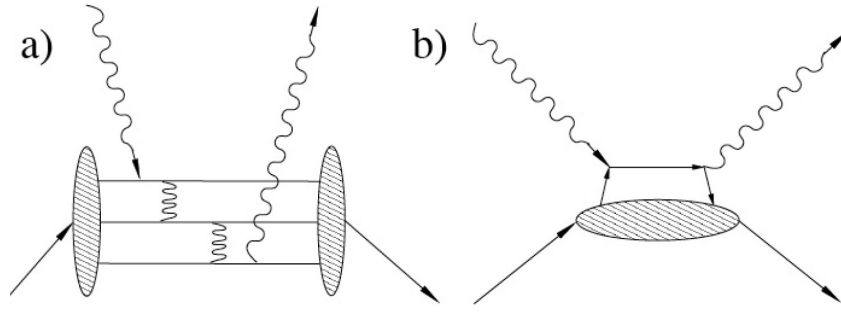


FIGURE 4. Diagrams for the $N \rightarrow N$ and $N \rightarrow \Delta$ processes for real and virtual Compton scattering at high energies. a) Momentum shared by many quarks due to gluon exchange; b) the handbag diagram- momentum absorbed by a single quark. The diagram with the incoming and outgoing photon lines crossed is not shown. Figure from [73].

Observation of non zero quark angular momentum in the proton has been demonstrated by the HERMES collaboration [Rith]. They have observed single spin asymmetries in semi-inclusive deep inelastic scattering DIS for transversely polarized proton targets. They measured non-zero Sivers distribution functions for semi-inclusive DIS with positive pions and kaons. The Sivers function describes the correlation between intrinsic quark transverse momentum p_T and transverse nucleon spin and requires orbital angular momentum in the nucleon to be non-zero [Rith].

The field of high energy deep inelastic scattering with polarization degrees of freedom has great potential to measure $L > 0$ angular momentum amplitudes in the nucleon. We are presently at the beginning of this very interesting development.

EXPERIMENTAL MEASUREMENTS AND INTERPRETATION

The experimental landscape concerning the investigation of shape of hadrons, until quite recently, has been to a large degree dominated by the quest for resonant quadrupole amplitudes in the $\gamma N \rightarrow \Delta$ transition. It is evident from the proceedings of this workshop that the situation is rapidly changing: other reactions have been suggested and some have been explored theoretically. Issues concerning the study of form factors and of GDPs have bearing on the issue and the theoretical framework is currently being developed. The possibility of studying the $\gamma N \rightarrow \Delta$ transition in neutrons or in a nuclear target has been raised and it may become technically feasible in the near future. In addition to the formidable technical difficulties that such a program faces, the theoretical framework to extract the above mentioned and admittedly important physics, needs to be further developed.

The $\gamma N \rightarrow \Delta$ Channel

As commented earlier the $\gamma N \rightarrow \Delta$ transition currently offers the only quantitative experimental test of theories and models that incorporate mechanisms which predict hadron deformation in general and that of the proton in particular. This avenue developed in the late eighties [77] has been pursued and refined both theoretically and experimentally over the last thirty years. The experimental landscape as it emerged in the intervening years can be classified according to the reaction channel probed and on how exclusive it is. The $\Delta^+(1232)$ can be excited by real or virtual photons and it can decay [76] by π^0 (66%) or π^+ (33%) or by gamma decay ($0.56 \pm 0.04\%$):

$$\gamma^* p \rightarrow \Delta^+(1232) \rightarrow p\pi^0 \quad (66\%)$$

$$\gamma^* p \rightarrow \Delta^+(1232) \rightarrow n\pi^+ \quad (33\%)$$

$$\gamma^* p \rightarrow \Delta^+(1232) \rightarrow p\gamma \quad (0.56\%)$$

where γ^* denotes the real (often polarized) or virtual photon inducing the excitation. The first two channels have been extensively explored while the third, involving the small gamma decay branch, has been studied with real compton scattering measurements (RCS). Virtual compton scattering measurements (VCS) on the $\Delta^+(1232)$ are just beginning

to emerge with the dual aim of either mapping the polarizabilities at high missing mass [88] and/or the issue of deformation [89].

It is possible to classify nucleon resonance photoproduction experiments by the exclusivity of the reaction channel studied. We classify the $\gamma N \rightarrow \Delta$ experiments (and nucleon resonance studies in general) as "first", "second" and "third" generation using such a criterion. We term "first generation" experiments those that established the reaction mechanisms and obtained the first data. We call second "generation experiments" those that have used high quality beams and polarization degrees of freedom either in the entrance or the exit channel. Finally we call "third generation" experiments those that employ double polarization degrees of freedom: either both in the entrance and exit channels or equivalently polarized beams and targets. The first generation experiments were conducted in the late sixties and early seventies before the issue of deformation was even raised- for an excellent review see the monograph by Amaldi, Fubini and Furlan [81]. These measurements were performed with low duty factor accelerators (DESY, NINA,CEA), low quality beams and with experimental equipment not designed to address such refined questions. The data that emerged, as far as the issue of deformation was concerned, were inconclusive, and limited by big systematic uncertainties and poor statistics, but they did provide valuable guidance on the design of the second generations experiments [83]. The second generation experiments were obtained by a newer generation machines (Brookhaven, Bates, MAMI, CEBAF) with optimized or especially designed equipment, such as the OOPS spectrometer at Bates, and in general with polarized beams. Third generation experiments are now beginning to emerge; they have been conducted primarily with real photons (polarized and tagged, impinging on polarized targets). Electroproduction experiments with polarized targets are particularly difficult with only one measurement reported in the literature using the internal target facility at NIKHEF [22], of low statistical accuracy. This experiment should be viewed as a valuable demonstration of an important technique. Recently the BLAST collaboration at Bates has measured the inclusive double-polarized response from hydrogen spanning the Δ region from 1100-1400 MeV and Q^2 from 0.08 to 0.3 GeV² with small systematic errors for the double asymmetry. This will allow them to obtain a good extractions of the CMR and EMR[58]. The recently reported JLab Hall A experiment [26] which presented high quality extensive recoil polarization measurements using polarized beams is truly third generation experiment which both demonstrated the feasibility of the technique, the precision that can be achieved and the rich physics output that can emerge. Unfortunately, no similar follow up measurements are scheduled for the immediate future.

In general, in the real photon sector the "second generation" experiments are completed and analyzed and the era of "third generation" experiments is about to begin in earnest, in view of the important instrumentation initiatives [84] at Mainz and at Bonn. In the electroproduction sector, data are still emerging from second generation experiments while experiments of third generation are just beginning to emerge. Jlab and MAMI C have optimal beams and detection systems for the pursuit of this program which is far from being exhausted.

The coincident $p(\vec{e}, e' \pi)$ cross section in the one-photon-exchange-approximation can be written as [68]:

$$\frac{d\sigma}{d\omega d\Omega_e d\Omega_\pi^{cm}} = \Gamma_\nu \sigma_h(\theta, \phi) \quad (8)$$

$$\sigma_h(\theta, \phi) = \sigma_T + \varepsilon \sigma_L + \sqrt{2\varepsilon(1+\varepsilon)} \sigma_{TL} \cos \phi$$

$$+ \varepsilon \sigma_{TT} \cos 2\phi + h p_e \sqrt{2\varepsilon(1-\varepsilon)} \sigma_{TL} \quad ,$$

where Γ_ν is the virtual photon flux, $h = \pm 1$ is the electron helicity, p_e is the magnitude of the longitudinal electron polarization, ε is the virtual photon polarization, θ and ϕ are the pion CM polar and azimuthal angles relative to the momentum transfer \vec{q} , and σ_L , σ_T , σ_{TL} , and σ_{TT} are the longitudinal, transverse, transverse-longitudinal, and transverse-transverse interference cross sections, respectively [68]. In the case of $p(\vec{\gamma}, \pi)$ the longitudinal responses are absent. The small quadrupole resonant quadrupole multipoles ($E_{1+}^{3/2}$) and ($S_{1+}^{3/2}$) have been investigated using the interference responses σ_{LT} and σ_{TT} , where the small amplitudes are exposed by interfering with the dominant M1 amplitude.

Real Photon Measurements

Precision measurements with polarized tagged photons performed at Mainz and Brookhaven (LEGS) in the late nineties have converged at the level of asymmetries resulting in a resonant EMR= $\text{Im}E_{1+}^{3/2}/\text{Im}M_{1+}^{3/2}$ of $(-3.0 \pm 0.3)\%$ [13] and $(-2.5 \pm 0.3)\%$ [12]. A number of theoretical calculations are in good agreement with the experimentally

derived EMR. However, important discrepancies still persist in the measurements of the two labs in the detailed angular and energy distributions. Both the (γ, π^0) and the (γ, π^+) channels have been studied extensively. (γ, γ) (RCS) has also studied [85], where the resonance pion-photoproduction amplitudes were evaluated leading to the multipole E2/M1 ratio $\text{EMR}(340 \text{ MeV}) = (-1.6 \pm 0.4_{(\text{stat}+\text{sys})} \pm 0.2_{(\text{model})})\%$, in reasonable agreement with the photopion measurements.

The "deformation" signal in the real photon sector comes from the study of the $E_{1+}^{3/2}$ (transverse quadrupole) multipole. The desired signal is particularly hard to isolate because the transverse channel is overwhelmed by the M_{1+} amplitudes and contaminated with other background processes of similar magnitude. In this sense, the $E_{1+}^{3/2}$ appears in next to leading order (NLO) in photoproduction. The impressive results from LEGS and MAMI are a tour de force of experimental finesse: they make the small quadrupole amplitude visible, as it can be seen in the right panel Figure 5, and they extracted with small systematic uncertainty by measuring the polarization asymmetry $\Sigma = (\sigma_{\parallel} - \sigma_{\perp}) / (\sigma_{\parallel} + \sigma_{\perp})$ which is measured by flipping the polarization of the tagged photon beam parallel (\parallel) and perpendicular (\perp) to the beam direction. It is exactly for this reason that we have convergence at the level of asymmetry but not at the level of cross sections. Analysis of the MAMI (γ, π^+) and (γ, π^0) data, yields the impressive results shown in the left panel of Figure 5. It is obvious from the figure that the derived results heavily depend on the W dependence of the cross section. It is also quite revealing that the $E_{1+}^{3/2}$ multipoles have a striking non resonant shape, a manifestation of the complicated processes that contribute to this channel, as discussed in <Drechsel>.

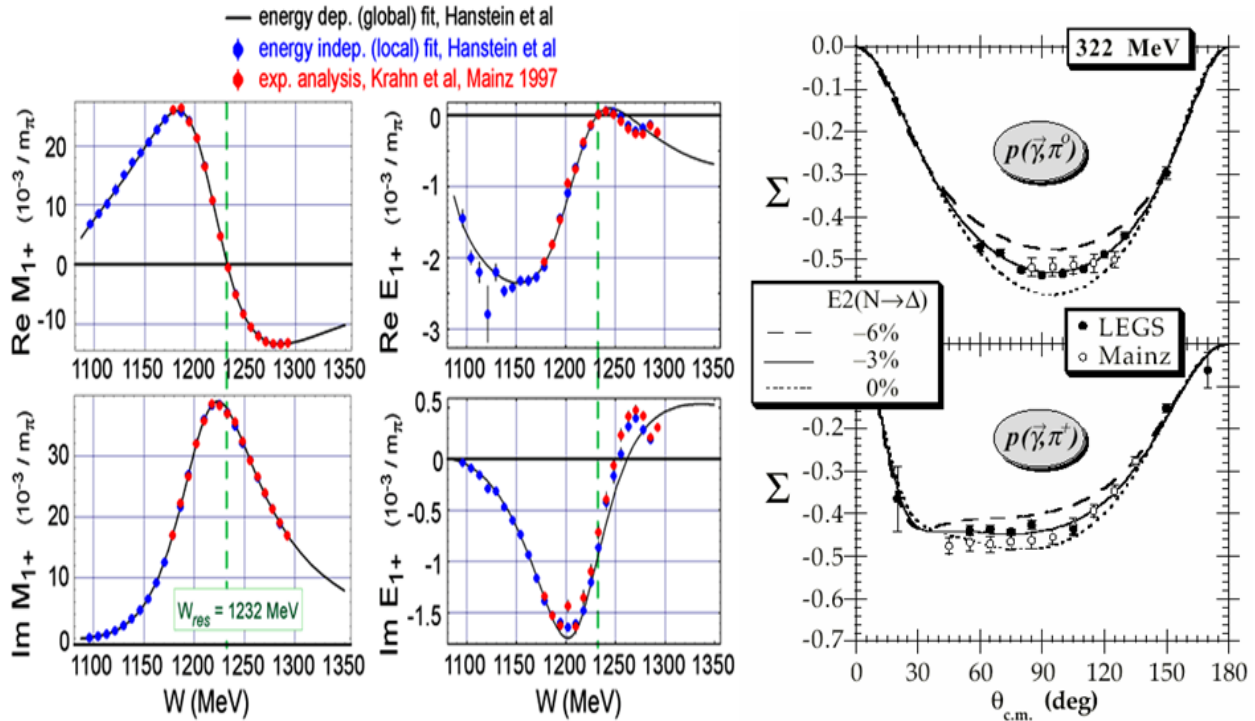


FIGURE 5. Measurements from MAMI and LEGS have yielded precise measurements of the resonant quadrupole amplitude at the photon point. A most sensitive probe is the polarization asymmetry $\Sigma = (\sigma_{\parallel} - \sigma_{\perp}) / (\sigma_{\parallel} + \sigma_{\perp})$ which has been measured precisely at both MAMI and LEGS. The derived multipoles from the Mainz cross sections, yield an accurate measurement of EMR.

The situation concerning the $\gamma N \rightarrow \Delta$ transition in the photon sector has remained stable, without experimental results reported to change this picture in the last five years. More recent analysis [78] and data <Kotula> which give $\text{EMR} = -2.74 \pm 0.03_{(\text{stat})} \pm 0.3_{(\text{sys})}$, confirm the EMR values of [13, 12]. However, in the closely related areas of threshold pion production [80] and in the measurement of the magnetic dipole [84, 82] of the $\Delta^+(1232)$ the very precise results that emerged are testing and providing valuable guidance to theory and phenomenology that is common to both. The recent installation of the crystal ball at MAMI and of the crystal Barrel in Bonn, have brought into existence new very powerful tools and as a result new more precise data and results can now be expected.

Electroproduction measurements

Electron scattering experiments offer a far richer field of study, in comparison to real photons, since in addition to the transverse responses the longitudinal responses are accessible which are sensitive to leading order to the $L_{1+}^{3/2}$. In addition to the W dependence the Q^2 evolution of the various responses can be studied as well. The Q^2 dependence offers, as is well known, the ability to distinguish between large scale and short scale process, of particular value in the quest to distinguish between the effects of the mesonic cloud from those of the quark core. These advantages are however hard to realize and time consuming due primarily to the numerous measurements needed to cover the widest possible range of momentum transfers. This explains the time lag with which electron scattering experiments have appeared: while the real photon measurements appear to have converged already at approximately around the year 2000, the electroproduction experiments are only now reaching a similar stage of maturity.

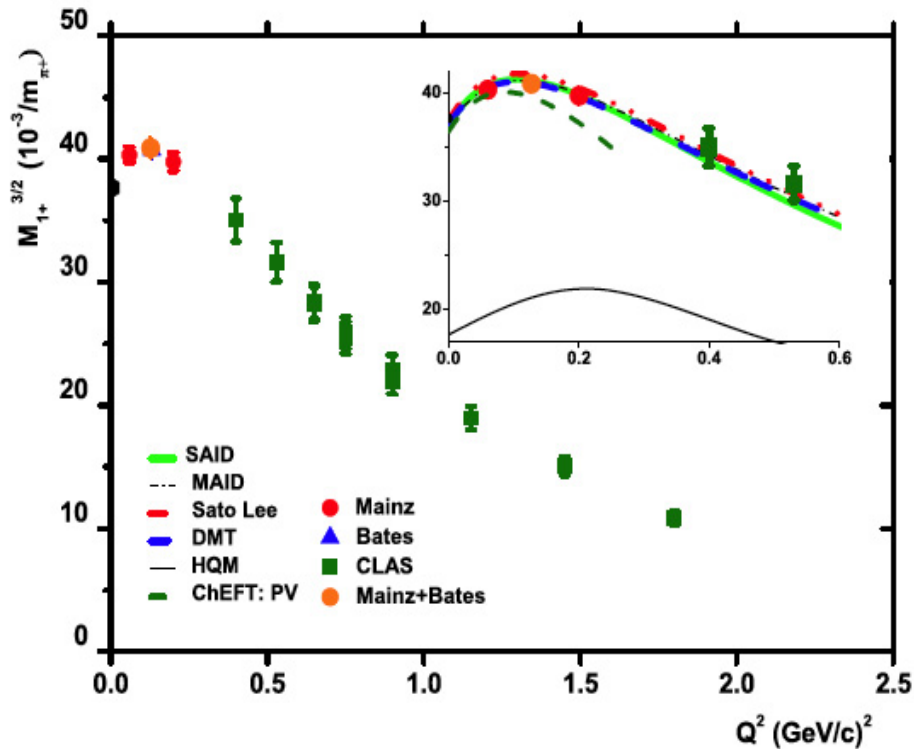


FIGURE 6. Experimentally derived M1 values compared to lattice and EFT results. The derived multipole ratios are generally shown without the model error that is of the order or larger than the depicted experimental error.

Results from several groups which are consistent and converging have been reported in [7] and in this volume. These experiments [15, 16, 21, 14, 20, 19, 24] at Bates, Bonn, MAMI and JLab have mapped the momentum transfer range from $Q^2 = 0.06$ to 6.0 $(\text{GeV}/c)^2$ with high precision in a limited number of sensitive observables. Earlier discrepancies between measurements from different labs have been resolved: There are no known outstanding discrepancies of relevance in electroproduction data, an achievement of the last few years. There are discrepancies at the extracted EMR and CMR values (which are not experimental observables) which are primarily due to the methodology that is used in extracting multipoles, as it will be discussed in the next section.

Starting from the experimental observables two methods have been used and are reported in the literature for extracting multipole amplitudes: a) In the Truncated Multipole Expansion (TME) approximation most or all of the non resonant multipoles are neglected (e.g. see [14, 20]) assuming that at resonance only the resonant terms contribute significantly, and b) In the Model Dependent Extraction (MDE) method a phenomenological reaction framework with adjustable quadrupole amplitudes is used to perform a model extraction (e.g. see [20, 16, 24]). It is assumed that the reaction is controlled at the level of precision required for the disentanglement of the background from the

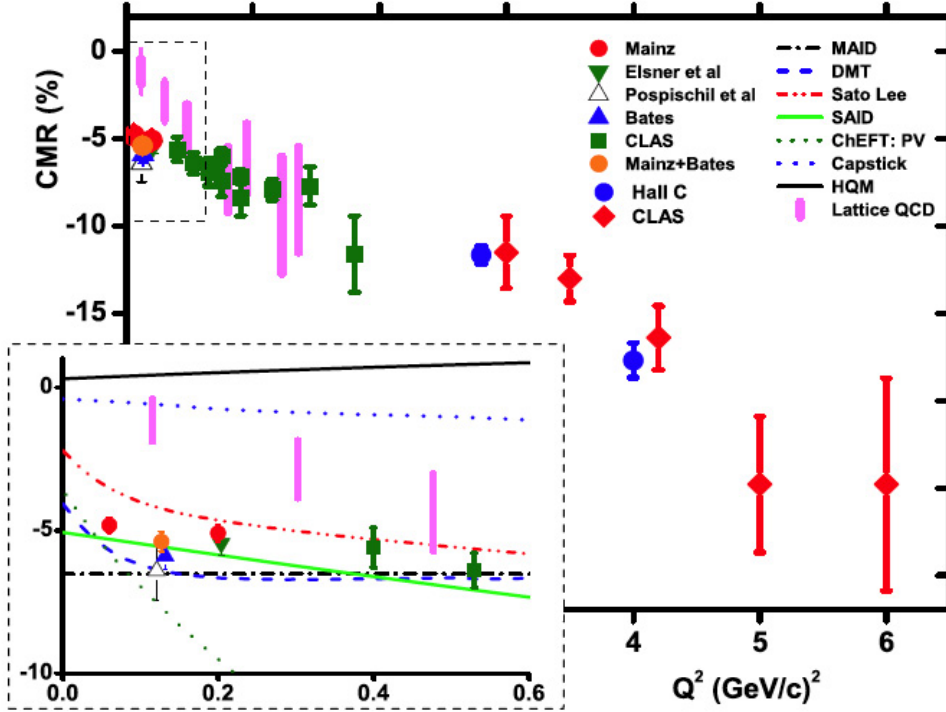


FIGURE 7. Experimentally derived CMR values compared to lattice and EFT results. The derived multipole ratios are generally shown without the model error that is of the order or larger than the depicted experimental error.

resonance. Clearly the MDE method is superior, given the sophistication that phenomenological models have achieved in describing the data, and as a result the TME method needs only be used to set a base line for the importance of the resonant terms and for the pedagogical value it offers.

In the recent electroproduction experiments which almost invariably are carried out with polarized beams, the TL and the TL' (transverse-longitudinal) response functions are the real and imaginary parts of the same combination of multipole amplitudes. In the S&P ($L_{max} = 1$) wave approximation they can be written as [68]:

$$\begin{aligned}
 \sigma_{TL}(\theta) &\simeq -\sin\theta \operatorname{Re}[A_{TL} + B_{TL} \cos\theta] \\
 \sigma_{TL'}(\theta) &\simeq \sin\theta \operatorname{Im}[A_{TL} + B_{TL} \cos\theta] \\
 A_{TL} &\simeq -L_{0+}^* M_{1+} \\
 B_{TL} &\simeq -6L_{1+}^* M_{1+}
 \end{aligned} \tag{9}$$

The two responses are particularly valuable because σ_{TL} is most sensitive to the presence of resonant quadrupole amplitudes while $\sigma_{TL'}$ is particularly sensitive to the background contributions, thus providing information on the two key experimental issues being explored and which need to be controlled independently. The importance of background is clearly seen in the W behavior of the responses [16] and the non-vanishing recoil polarization P_n [15, 21], which bear close resemblance to the fifth response.

The TT (Transverse- Transverse) response which is sensitive to the electric quadrupole amplitude, and which is the primary source of information for the EMR at the photon point was only recently isolated for the first time at non-zero Q^2 has in the last five years been vigorously pursued at Bates, Jlab and MAMI [86, 87]. The response functions σ_T and σ_{TT} contain the term $\Re[E_{1+}^* M_{1+}]$ but also the dominant term $|M_{1+}|^2$. The influence of the dominant $|M_{1+}|^2$ term can be diminished by measuring the following combination of the σ_T and σ_{TT} responses:

$$\begin{aligned}
 \sigma_{E2}(\theta_{pq}^*) &= \sigma_T(\theta_{pq}^*) + \sigma_{TT}(\theta_{pq}^*) - \sigma_T(0) \simeq \\
 &2\Re[E_{0+}^* (3E_{1+} + M_{1+} - M_{1-})] (1 - \cos\theta_{pq}^*)
 \end{aligned}$$

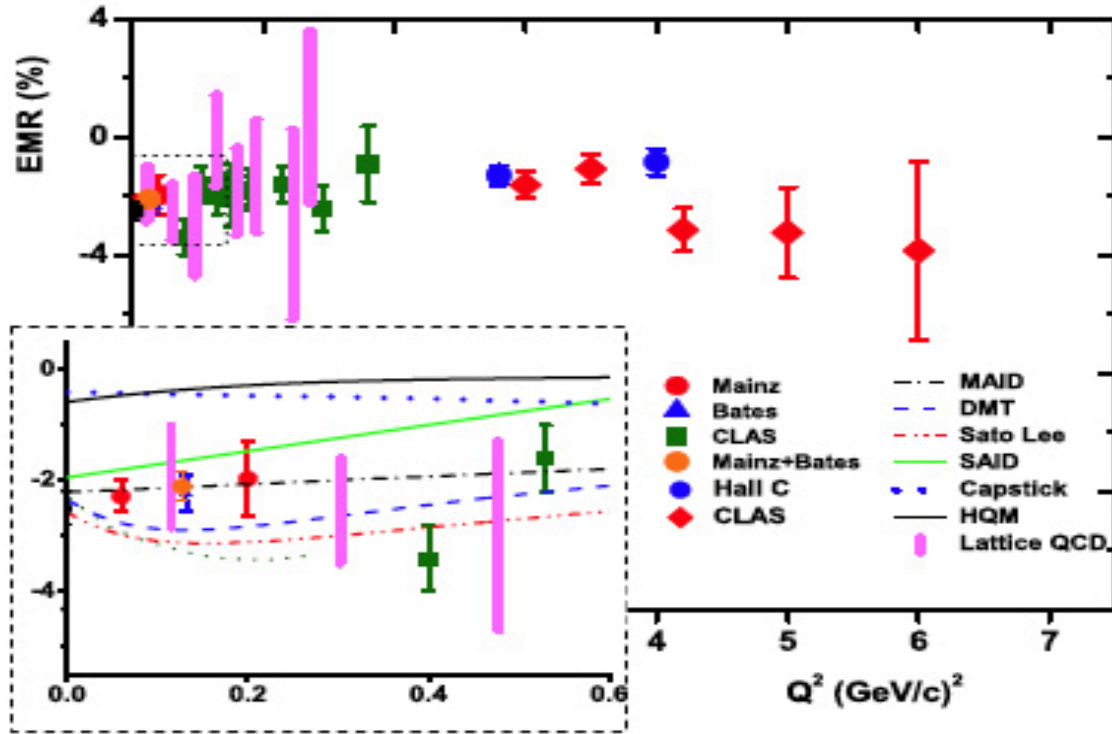


FIGURE 8. Experimentally derived EMR values compared to lattice and EFT results. The derived multipole ratios are generally shown without the model error that is of the order or larger than the depicted experimental error.

$$-12\Re[E_{1+}^*(M_{1+} - M_{1-})] \sin 2\theta_{pq}^* \quad (10)$$

The term of interest $\Re[E_{1+}^*M_{1+}]$ is enhanced by a factor of twelve (12) while the leading term ($|M_{1+}|^2$) is eliminated [8]! This has been used as a tool to extract a most precise measurements of EMR [18, 25].

As the $\gamma^*N \rightarrow \Delta$ data became more accurate it was generally recognized that the quark model predictions did not agree with the data. In particular the dominant M1 matrix element was predicted to be $\simeq 30\%$ low and the E2 and C2 amplitudes are generally at least an order of magnitude too small and often of the wrong sign as shown in Figs. 7 and 8. As was discussed in the introduction it was soon realized that the pion cloud needed to be added to quark models. This failure is to be expected since the quark model does not respect chiral symmetry whose dynamic breaking leads to a strong, non-spherical, pion cloud around all hadrons [9]. It was shown by the calculations of the Sato-Lee [38] and DMT [39] models that most of the strength of the responses (and the EMR and CMR) at very low Q^2 values (below $\simeq 0.25 \text{ GeV}^2/c^2$) arises on account of the mesonic degrees of freedom. Finally this has been theoretically confirmed by the chiral effective field theory calculations <Gail-Hemmert, Pascalutsa-Vanderhaeghen> [34, 33]. The recent results from MAMI along with the earlier ones from Bates [86] and the recent low Q^2 measurements from CLAS [87], give strong support to this interpretation.

Figures 7 and Fig. 8 offer a recent compilation of the current status of CMR and EMR as a function of Q^2 . It can be observed that both EMR and CMR are small and negative in the region where they have been measured. At asymptotic values of Q^2 helicity conservation [90] requires that $\text{EMR} \rightarrow 1.0$ and that $\text{CMR} \rightarrow \text{constant}$. Clearly this regime has not been reached. The upgrade of CEBAF to 12 GeV offers hope that the measurements will be extended to higher Q^2 , although this will pose significant challenges in isolating the relevant partial cross sections and even bigger ones in extracting the relevant amplitudes.

Finally, important is the investigation of the $H(\vec{e}, e'p) \gamma$ channel which has not been exploited experimentally yet.

The dispersion theory [91] of the Mainz group, taken in conjunction with the previous work of Vanderhaegen et al. [92] allows to address the physics of "deformation" and of nucleon polarizabilities in the region above pion threshold simultaneously. Very recent results from Mainz report the extraction of polarizabilities [88] and the first observation of VCS data sensitive to the resonant quadrupole amplitudes [89]. Extraction of the quadrupole amplitudes through VCS opens a new vista which can provide important cross checks to the derived results from the pionic channel.

Sensitivity, Precision and Estimation of Uncertainties

The progress achieved in the last few years in the experimental investigation of the issue of deformation is truly outstanding. In the $\gamma N \rightarrow \Delta$ investigations data up to $Q^2 = 6.0$ (GeV/c)² are in general characterized by small systematic error and high statistical precision. The sensitivity of the data to the issue of deformation had at about the same time been demonstrated, and as a result, the research thrust shifted from the investigation of whether the conjecture for deformation was valid to the exploration of the mechanisms that cause it. The implications of this shift had profound effect on the accuracy demanded from both the experiment and the theoretical calculations. Investigating the physical origin of deformation requires the comparison of theoretical results with experimentally derived quantities, such as multipole amplitudes at a much higher level of precision. A number of models and recently lattice results are in qualitative agreement with the data and amongst themselves. Understanding the mechanisms that cause deformation requires distinguishing among successful descriptions that emphasize different aspects of the same basic process. This in turn necessitates a precise statement on the uncertainties that characterize both the experimental results and the theoretical calculations to which they are compared.

The situation described above is reminiscent of the "crisis" in the analysis of elastic electron scattering data in the early seventies, where the very precise electron scattering data that were emerging could not be meaningfully compared with the theoretical calculations of the time (primarily nuclear mean field theories) at the level of charge densities. This was primarily due to the lack of appropriate methodology which could enable the quantification of uncertainties in the extracted densities, which are not experimental observables. The resolution of that "crisis" through the introduction of a "Model Independent" extraction of charge densities led to a revolution in the field and to the outstanding achievements in elastic and inelastic scattering of the seventies and eighties.

In the quest for understanding of deformation through the $\gamma N \rightarrow \Delta$ transition, a comparison is made to multipole amplitudes or their ratios (EMR and CMR) which are also derived quantities not experimental quantities. A quantification of the uncertainties that characterize them is difficult but essential. Early estimates showed that indeed the error uncertainty was in a number of cases dominant. It is also the case that theoretical calculations that predict them need to provide not only central values but an uncertainty as well. This is rarely done; even in the case of lattice calculations, the quoted errors are statistical not systematic and certainly not model. In the few cases where this was done the associated uncertainty is quite large.

The leading method of extraction of multipole amplitudes, the Model Dependent Extraction (MDE), results in extracted values that are biased by the model. The principal drawback of this method is that the derived results are characterized by a had to estimate model error, especially if a single model is employed [19, 20, 21, 22, 23, 27] in the extraction. An ansatz for estimating the model uncertainties in the extracted multipoles has been proposed [8] and has been used in a few cases [18, 24]. In this method the same data are analyzed employing different models which describe the data adequately, and attributing the resulting spread in the extracted quantities to model uncertainty. A critical assessment of this approach in the case of the $N \rightarrow \Delta$ transition and the resulting uncertainties is presented in reference [93]. It is convincingly demonstrated that the models currently available of considerable sophistication provide though a MDE a convergent method of extracting resonant amplitudes, at least at low Q^2 . The role of the small non resonant amplitudes, which in MDE are fixed by the model, is explored in detail. It is found that while each one of them may be of little significance they collectively could induce large correlations and that intrinsic model error is similar in size to the model-to-model error. This thorough investigation concludes that MDE, which constitutes the most advanced available methodology, "without improvement in the models, this is as far as the current data can take us".

In an attempt to address the same fundamental issue a novel method for extracting multipole information from experimental nucleon resonance data was presented in the workshop [94]. The Athens Model Independent Analysis Scheme (AMIAS) is designed to be a rigorous, precise, and model independent scheme and holds the promise to be a new tool for nucleon resonance analysis with important consequences. The analysis of the particular data discussed in the paper, is demonstrated to yield new information on background amplitudes, which MDE is incapable

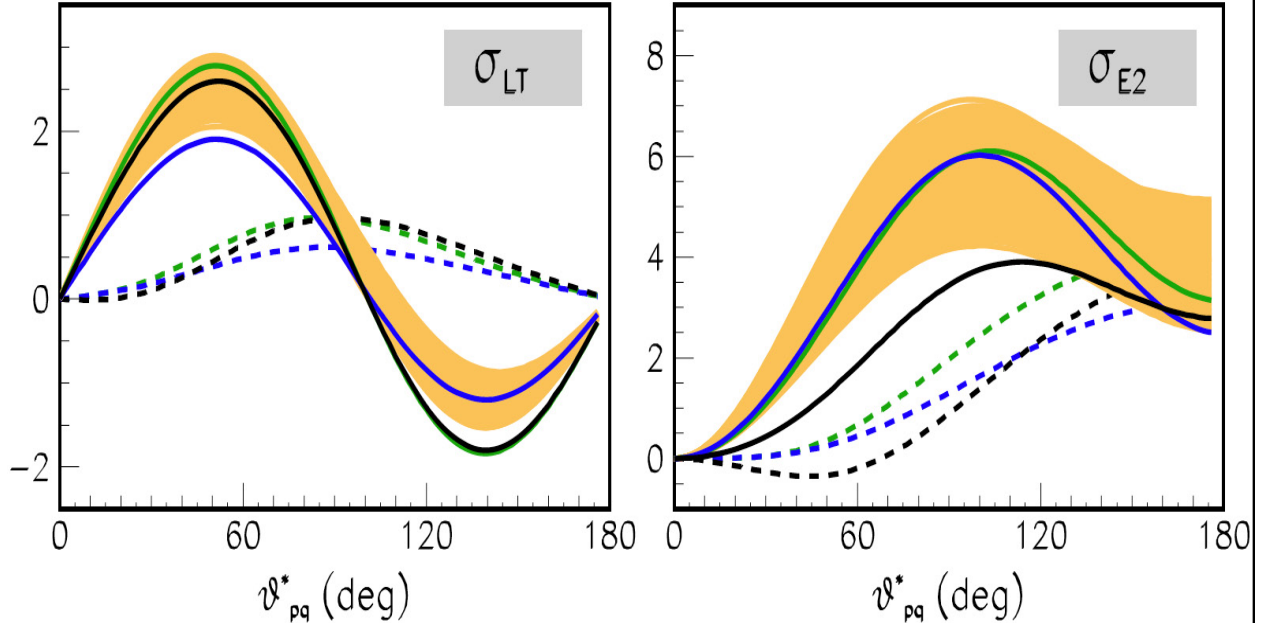


FIGURE 9. The precise range of uncertainty that is allowed by the $Q^2 = 0.127 \text{ (GeV/c)}^2$ Bates and Mainz data for the σ_{LT} and σ_{E2} responses is shown as a function of θ_{pq}^* . Current theoretical models (MAID in black, SL in blue and DMT in green) predict this satisfactorily within a 2σ confidence level. No "spherical" description (same color coding for the various models but with dashed curves) of the nucleon can describe the data; they are excluded with high confidence.

of accessing [93]. A very distinct and promising aspect of the AMIAS method is its ability to quantify the uncertainty of the extracted multipoles.

Results from AMIAS are shown Figure 9 concerning the CMR sensitive σ_{LT} and the EMR sensitive σ_{E2} partial cross sections with the precisely defined 1σ (68%) uncertainty. The experimentally allowed σ_{LT} and σ_{E2} partial cross sections, as constrained by the $Q^2 = 0.127 \text{ (GeV/c)}^2$ Bates and Mainz data, are shown as function of θ_{pq}^* . They are compared with theoretical model predictions that account for them. It is evident that the model predictions (dotted curves) with resonant quadrupole amplitudes set to zero, which amounts to spherical solutions, are excluded with high confidence. The "deformed" model predictions, if we assume that they are characterized by negligible model error, are in agreement at the 2σ level, which will allow their characterization as reasonable. Differences among the various model are visible, however commenting on their differences would be far more meaningful, if their model error was known. The above comments notwithstanding, the potential of AMIAS is evident. The comparison that it offers demonstrates once again that the assumption of sphericity for both the nucleon and the $\Delta^+(1232)$ is incompatible with the data.

SUMMARY AND CONCLUSION

In this workshop the physical basis of the deviation of hadron shapes, and in particular those of the nucleon and Δ , from spherical symmetry (non-spherical amplitudes) has been addressed including the experimental methods and results. At the present time the only quantitative method experimentally accessible is through the investigation of the $\gamma^*p \rightarrow \Delta$ reaction, and the workshop focused on this. In addition attention was paid to emerging new approaches using high energy probes. A promising method for which the theoretical framework has been rapidly developing in recent years uses deeply virtual Compton scattering and hard exclusive meson production to obtain generalized parton distributions <Vanderhaeghen, Kroll>. In addition semi-inclusive deep inelastic scattering experiments with transverse polarized beam and target also are beginning to show the effect of non-zero quark angular momentum (non-zero Sivers effect) <Rith>.

After over a decade of intense work in many laboratories on the $\gamma^*N \rightarrow \Delta$ reaction, the experiments have reached a high level of sensitivity for the non-spherical electric(E2) and Coulomb quadrupole(C2) amplitudes; these have been

observed with good precision as a function of Q^2 from the photon point [12, 13] through 6 GeV^2 [Sparveris, Smith, Ungaro] [15]- [27]. For the highest Q^2 values it has been observed that the asymptotic QCD predictions have not yet been reached [Ungaro] [27]. Lattice QCD [Alexandrou] [30] with the appropriate chiral extrapolations to the physical pion mass are in reasonable agreement with experiment [Pascalutsa-Vanderhaeghen] [34, 11]. However, due to the high pion masses that are used in lattice calculations, and also the limited accuracy of the present chiral extrapolations, the theoretical errors are much larger than the experimental ones. Therefore further theoretical work is required to make this comparison quantitative.

For the $\gamma^* N \rightarrow \Delta$ reaction at $Q^2 \leq 1 \text{ GeV}^2$ the pion cloud is the dominant contributor to the quadrupole amplitudes. This first became clear when quark model calculations for the quadrupole amplitudes were shown to be at least an order of magnitude too small and even have the wrong sign [Sparveris, Smith] [18, 24, 25]. On the other hand effective chiral field theory [Gail-Hemmer, Pascalutsa-Vanderhaeghen] [32, 33, 34, 11], and dynamic model calculations [Drechsel-Tiator] [38, 39] which include the effects of the pion-cloud are in approximate agreement with experiment. This is expected due to the spontaneous hiding (breaking) of chiral symmetry in QCD and the resulting, long range (low Q^2), effects of the pion-cloud.

In recent years there has been considerable progress in the measurement of nucleon form factors by electron scattering including polarization degrees of freedom [de Jager]. These include polarized electron scattering from polarized targets and also detection of recoil nucleon polarization. There has also been excellent progress in the measurement of virtual Compton scattering. The results for nucleon form factors [de Jager] and virtual Compton scattering [Miskimen] [65] experiments indicate that the pion-cloud is playing a significant role in nucleon structure. It has been demonstrated that the concept of the pion cloud is very interesting qualitatively but it cannot be quantified in a model independent way [Meissner] [57].

There has been a considerable amount of work to improve the extraction of the quadrupole amplitudes from the experimental cross sections in the $ep \rightarrow \pi N$ reaction in the Δ region. Empirical extractions of the multipole amplitudes have considerably improved due to the increasing sophistication and accuracy of both the experiments and the reaction models [Drechsel-Tiator, Arndt] [38, 39, 70, 50]. A systematic comparison of results obtained by the different models indicates that the model errors are comparable to the experimental errors [Stave] [18, 24, 25]. However, discriminating between successful competing models or theoretical approaches, which is necessary in order to allow an understanding of the detailed mechanisms that generate non spherical components (amplitudes) in the hadron wavefunctions, requires even more accurate experimental data and more precise analysis tools. Towards this direction, the new method (AMIAS) for extracting model independent multipoles from experiment which was presented for the first time at this workshop [Stiliaris-Papanicolas], is an important first development.

Last, but not least, we believe that we can look forward to exciting new developments in the determination of non-zero angular momentum studies of hadrons, particularly the proton. These will most likely include a new generation of high energy probing as well as further refinements in the $\gamma^* N \rightarrow \Delta$ reaction.

REFERENCES

1. S. L. Glashow, *Physica* **A96**, 27–30 (1979).
2. A. de Rujula, H. Georgi and S.L. Glashow *et al.*, *Phys. Rev* **D12**, 147 (1975).
3. W. Heisenberg, *Z. Phys.* **39**, 499 (1926); G. Breit, *Phys. Rev.* **36**, 383 (1930), and E. Fermi, *Z. Phys.* **60**, 320 (1930).
4. N. Isgur, G. Karl and R. Koniuk, *Phys. Rev.* **D25**, 2394 (1982).
5. R. Carlitz, S.D. Ellis, and R. Savit, *Phys. Lett.* **64B**, 1081 (1977). N. Isgur, *Acta Phys. Pol.* **B8**, 1081 (1977).
6. N. Isgur, G. Karl, and D.W.L. Sprung, *Phys. Rev.* **D23**, 163 (1981).
7. D. Drechsel, and L. Tiator, editors, *Proceedings of the Workshop on the Physics of Excited Nucleons*, World Scientific, 2001.
8. C. N. Papanicolas, *Eur. Phys. J.* **A18**, 141–145 (2003).
9. A. M. Bernstein, *Eur. Phys. J.* **A17**, 349–355 (2003).
10. V.D. Burkert and T.S.H. Lee, *Int.J.Mod.Phys.* **E13**, 1035 (2004).
11. Vladimir Pascalutsa, Marc Vanderhaeghen, and Shin Nan Yang, *Phys. Rep.* **437**, 125 (2007).
12. R. Beck, *et al.*, *Phys. Rev.* **C61**, 035204 (2000).
13. G. Blaupied, *et al.*, *Phys. Rev.* **C64**, 025203 (2001).
14. F. Kalleicher *et al.*, *Z. Phys.* **A359**, 201 (1997).
15. G. A. Warren, *et al.*, *Phys. Rev.* **C58**, 3722 (1998).
16. C. Mertz, *et al.*, *Phys. Rev. Lett.* **86**, 2963–2966 (2001).
17. C. Kunz, *et al.*, *Phys. Lett.* **B564**, 21–26 (2003).
18. N. F. Sparveris, *et al.*, *Phys. Rev. Lett.* **94**, 022003 (2005).
19. K. Joo, *et al.*, *Phys. Rev. Lett.* **88**, 122001 (2002).

20. V. V. Frolov, et al., *Phys. Rev. Lett.* **82**, 45–48 (1999).
21. T. Pospischil, et al., *Phys. Rev. Lett.* **86**, 2959–2962 (2001).
22. P. Bartsch, et al., *Phys. Rev. Lett.* **88**, 142001 (2002).
23. D. Elsner, et al., *Eur. Phys. J.* **A27**, 91–97 (2006).
24. S. Stave, et al., *Eur. Phys. J.* **A30**, 471(2006), nucl-ex/0604013.
25. N.F. Sparveris, et al., nucl-ex/0611033.
26. J.J. Kelly et al, *Phys.Rev.Lett.* **95**,102001(2005), nucl-ex/0509004.
27. M. Ungaro, M. et al.,*Phys. Rev. Lett.* **97**, 112003 (2006).
28. G. Kaelbermann and J. M. Eisenberg, *Phys. Rev. D* **28**, 71 (1983).
29. S. Capstick, and G. Karl, *Phys. Rev.* **D41**, 2767 (1990); S. Capstick and W. Roberts, *Prog. Part. Nucl. Phys.* **45**, S241(2000).
30. C. Alexandrou et al., *Phys. Rev. Lett.* **94**,021601(2005); *Phys. Rev. D* **69**, 114506 (2004).
31. M. Guidal, M.V. Polyakov, A.V. Radyushkin, M. Vanderhaeghen, *Phys.Rev.* **D72**:054013,2005.
32. G.C. Gellas, T.R. Hemmert, C.N. Ktorides and G.I. Poulis, *Phys. Rev.* **D60**:054022 (1999).
33. T. A. Gail, and T. R. Hemmert (2005), nucl-th/0512082.
34. V. Pascalutsa, and M. Vanderhaeghen, *Phys. Rev. Lett.* **95**, 232001 (2005); *Phys. Rev.***D73**, 034003 (2006).
35. D. Drechsel and M.M. Giannini, *Phys. Lett.* **143B**,329(1984); M. Bourdeau and N.C. Mukhopadhyay, *Phys. Rev. Lett.* **58**, 976(1987).
36. K. Bermuth, D. Drechsel, L. Tiator and J. B. Seaborn, *Phys. Rev.* **D37**, 89 (1988).
37. D. H. Lu, A. W. Thomas and A. G. Williams, *Phys. Rev.* **C55**, 3108 (1997).
38. T. Sato, and T. S. H. Lee, *Phys. Rev.* **C63**, 055201 (2001).
39. S. S. Kamalov, et al., *Phys. Lett.* **B522**, 27–36 (2001).
40. M. Fiolhais, B. Golli and S. Sirca, *Phys. Lett. B* **373**, 229 (1996).
41. A. J. Buchmann, E. Hernandez and A. Faessler, *Phys. Rev. C* **55**, 448 (1997).
42. P. Grabmayr and A. J. Buchmann, *Phys. Rev. Lett.* **86**, 2237 (2001). A. J. Buchmann, *Phys. Rev. Lett.* **93**, 212301 (2004).
43. A. J. Buchmann, J. A. Hester and R. F. Lebed, *Phys. Rev.* **D66**, 056002 (2002).
44. B.T. Feld, Models of Elementary Particles, Blaisdell Publishing Co., Waltham, Mass (1969).
45. A. J. Buchmann and E. M. Henley, *Phys. Rev.* **C63**,015202(2001)
46. Gerald A.Miller, *Phys. Rev.* **C68**,022201(2003).
47. Alexander Kvinikhidze, and Gerald A.Miller, *Phys. Rev.* **C73**,014007(2006).
48. B.W. Filippone, and X.D. Ji, *Adv. Nucl. Phys.* **26**, 1(2001).
49. D. Drechsel, O. Hanstein, S. S. Kamalov, and L. Tiator, *Nucl. Phys.* **A645**, 145–174 (1999).
50. R. A. Arndt, et al., *Phys. Rev.* **C66**, 055213 (2002), <http://gwdac.phys.gwu.edu>.
51. W.M. Yao et al., *Journal of Physics* **G33**, 1(2006).
52. Charles Earl Hyde-Wright and Kees de Jager, *Ann. Rev. Nucl. Part. Sci.*,**54**, 217 (2004).
53. M. De Sanctis, M.M. Giannini, E. Santopinto. and A. Vassallo, nucl-th/0506033 (2005).
54. H. W. Hammer, *Eur. Phys. J.* **A28**, 49 (2006), hep-ph/0602121.
55. M.A. Belushkin, H.W. Hammer, and U.G. Meissner, *Phys.Rev.* **C75**,035202(2007).
56. J. Friedrich and Th. Walcher, **EPJA17**, 607(2003).
57. H.W. Hammer, D. Drechsel, and U.G. Meissner, *Phys. Lett.* **B586**, 291(2004).
58. M. Kohl, private communication.
59. . James J. Kelly, *Phys.Rev.***C66**,065203(2002).
60. A. Faessler et al., *Phys. Rev.* **D73**, 074010(2006).
61. A. Faessler et al., *Phys. Rev.* **D74**, 114021(2006).
62. E.L. Lomon, *Phys. Rev.*, **64**, 035204 (2001); **PRC 66**, 045501(2002).
63. Franz Gross, Peter Agbakpe, *Phys. Rev.* **C73**, 015203(2006).
64. Franz Gross, G. Ramalho, M.T. Pena, nucl-th/0606029
65. P. Bourgeois, et al., *Phys. Rev. Lett.* **97**, 212001(2006)
66. V. Bernard, N. Kaiser, and U-G Meissner, *Phys. Rev. Lett.* **67**, 1515(1991).
67. T.R. Hemmert et al., *Phys. Rev.* **D62**, 014013(2000).
68. D. Drechsel, and L. Tiator, *J. Phys.* **G18**, 449 (1992). A. S. Raskin, and T. W. Donnelly, *Ann. Phys.* **191**, 78 (1989).
69. A.M.Bernstein, *Phys. Lett.* **B442**, 20(1998).
70. D. Drechsel, O. Hanstein, S. S. Kamalov, and L. Tiator, *Nucl. Phys.* **A645**, 145–174 (1999).
71. I.G. Aznauryan, *Phys. Rev.* **C67**, 015209 (2003).
72. D.J.Hamilton et al., *Phys.Rev. Lett.* **94**, 242001(2005).
73. C. Munoz Camacho et al., *Phys. Rev. Lett.* **97**, 261002 (2006).
74. Xiang-dong Ji, *Phys.Rev.Lett.* **78**,610(1997)
75. Xiang-dong Ji, *Phys.Rev.Lett.* **91**, 062001(2003). Andrei V. Belitsky, Xiang-dong Ji, Feng Yuan, *Phys.Rev.* **D69**, 074014(2004).
76. "Review of Particle Physics- PDG" W-M Yao et al 2006 *J. Phys. G: Nucl. Part. Phys.* **33** 1(2006)
77. G. Adams, N. Mukhopadhyay and P. Stoler, eds, *Proceedings of the Workshop on Excited Baryons*, World Scientific, 1989.
78. R.A. Arndt et al (BRAG), nucl-th/0106059 in ref.7
79. *Eur. Jour. of Phys.* **A21** 323 (2004)
80. *Eur. Jour. of Phys.* **A28** 129 (2006)
81. **Pion-electroproduction** E Amaldi, S Fubini, G Furlan, Springer Tracts Mod.Phys.,83 (1979).

82. M. Kotula, *Phys. Rev. Lett.* **89**, 2722001(2002).
83. C.N. Papanicolas in *Proceedings of the Workshop on Excited Baryons*, G. Adams, N. Mukhopadhyay and P. Stoler, eds, World Scientific, 1989.
84. M. Kotula, these Proceedings, Shape of Hadrons, Athens 2006.
85. G. Galler et.al *Phys. Lett.* **B503** (2001) 245-255
86. These Proceedings, Shape of Hadrons, Athens 2006.
87. These Proceedings, Shape of Hadrons, Athens 2006.
88. I.K. Bensafa, et al., To be published, hep-ph/0612248.
89. N. Sparveris, et al., private Communication(2006)and to be published.
90. C.E. Carlson and J.L. Poor *Phys. Rev.* **D38**, 2758 (1988)
91. B. Pasquini, *et al. Eur.Phys.J.* **A11** (2001) 185-208.
92. M. Vanderhaeghen *Nucl. Phys.* **A595**, 219 (1995).
93. S. Stave, A. M. Bernstein and I. Nakagawa, these Proceedings, Shape of Hadrons, Athens 2006.
94. E. Stiliaris and C.N. Papanicolas, these Proceedings, Shape of Hadrons, Athens 2006.

ACKNOWLEDGMENTS

We acknowledge the help we received from many colleagues who to varying degree helped in the preparation of this manuscript; this list certainly includes a good fraction of the hundred or so physicists that participated in the two (Athens and MIT) workshops. We are particularly indebted to C. Alexandrou, V. Brown, U-G. Meissner, N. Sparveris S. Stave, E. Stiliaris and M. Vanderhaegen for the help and the critical comments we received from them. Finally we would like to thank Gerry Miller for suggesting the title "Shape of Hadrons" for the second workshop, which we adopted as the title of this volume.

We would also like to thank the hosts of the two workshops. For the 2006 workshop the Institute of Accelerating Systems and Applications (IASA) and the National and Capodistrian University of Athens (NCUA). For the 2004 workshop the Laboratory for Nuclear Science and Bates Linear Accelerator Center of the Massachusetts Institute of Technology (MIT).